Inorganic Chemistry

pubs.acs.org/IC Article

Benzimidazole-diamide (bida) Pincer Chromium Complexes: Structures and Reactivity

Ann K. Kayser, Peter T. Wolczanski,* Thomas R. Cundari, Samantha N. MacMillan, and Melissa M. Bollmeyer



Cite This: Inorg. Chem. 2023, 62, 15450-15464



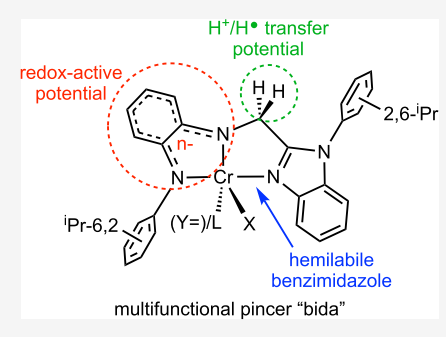
ACCESS I

III Metrics & More

Article Recommendations

Supporting Information

ABSTRACT: Serendipitous discovery of bida (i.e., $N^1-Ar-N^2-((1-Ar-1-benzo[d]-imidazol-2-yl)methyl)benzene-1,2-diamide; Ar = 2,6-iPr-C₆H₃), a potentially redox noninnocent, hemilabile pincer ligand with a methylene group that may facilitate proton/H atom reactivity, prompted its investigation. Chromium was chosen for study due to its multiple stable oxidation states. Disodium salt (bida)Na₂(THF)_n was prepared by thermal rearrangement of (dadi)Na₂(THF)₄ (i.e., (N,N'-di-2-(2,6-diisopropylphenylamine)phenylglyoxaldiimine)-Na₂(THF)₄). Salt metathesis of (bida)-Na₂(THF)_n (generated in situ) with CrCl₃(THF)₃ or Cl₃V=NAr (Ar = 2,6-iPr₂C₆H₃) afforded (bida)CrCl(THF) (1-THF) and (bida)CIV=NAr, respectively. Substitutions provided (bida)CrCl(PMe₂Ph) (1-PMe₂Ph) and (bida)CrR(THF) (2-R, where R = Me, CH₂CMe₂Ph (Nph)). Oxidation of 1-THF with ArN₃ (Ar = 2,6-iPr₂C₆H₃) or AdN₃ (Ad$



= 1-adamantyl) generated (bida)ClCr=NAr (3=NAr) and (bida)ClCr=NAd (3=NAd) and subsequent alkylation converted these to (bida)R'Cr=NR (R' = Me, R = Ad, Ar, 5=NR; R' = CH₂CMe₂Ph (Nph), R = Ad, Ar, 6=NR). In contrast, the addition of AdN₃ to 2-Nph gave the insertion product (bida)Cr(κ^2 -N,N-ArN₃Nph) (7). Addition of N-chlorosuccinimide to 1-THF produced (bia)CrCl₂(THF) (8), where bia is the pincer derived via hydrogen atom loss from bida methylene. A similar HAT afforded (bia)ClCr(CNAr')₂ (9, Ar' = 2,6-Me₂C₆H₃) when 3=NAd was exposed to Ar'NC. An empirical equation of charge was applied to each bida species, whose metric parameters are unchanging despite formal oxidation state conversions from Cr(III) to Cr(V). Calculations and Mulliken spin density assessments reveal several situations in which antiferromagnetic (AF) coupling and admixtures of integer ground states (GSs) describe a complicated electronic structure.

■ INTRODUCTION

Explorations in these laboratories have focused on varied expressions of redox noninnocence (RNI) in first row transition metal complexes, predominately chelates and in C–C bond forming processes. Expansion of the redox capability of base metals is a critical feature of RNI ligands that can potentially be used to circumvent deleterious 1e⁻ processes.

In many cases, metric parameters allow distinctions between metal and ligand redox states and correlated chemical reactivity. For example, Wieghardt et al. have interpreted the metrics pertaining to neutral (0), anionic (-1), and dianionic (-2) pyridine-imines through multiple crystallographic characterizations in conjunction with spectroscopy: dN(im)-C(im) = 1.28 (0), 1.34 (-1), 1.46 (-2) Å; dC(im)-C(py) = 1.47 (0), 1.41 (-1), 1.35 (-2) Å; dN(py)-C(py) = 1.35 (0), 1.39 (-1), 1.40 (-2) Å. 20,21 These metrics enabled the remarkable discovery of two independent molecules of $(dmpPI)_2FeBr$ ($dmpPI = \{2-py-CH=N(2,6-Me_2-C_6H_3)\}$), each differing in their electronic ground state: 1) a high spin $S_T = 3/2$ electromer resulting from an S = 2 iron core antiferromagnetically coupled (AF) to an S = 1/2 PI ligand, i.e., $(dmpPI)(dmpPI)^{-1}Fe^{\uparrow\downarrow\uparrow\uparrow\uparrow\uparrow}Br$ and 2) a low spin $S_T = 1/2$

electromer resulting from an S=1 iron core antiferromagnetically coupled (AF) to an S=1/2 PI ligand, i.e., (dmpPI)- $(dmpPI)^{-1}Fe^{1\downarrow\uparrow\downarrow\uparrow\uparrow}Br$.

Structural and reactivity studies of a tetradentate *bis*-aryldiamide-diimine ligand derived from $[\{-CH=N(1,2-C_6H_4)NH(2,6^{-i}Pr_2C_6H_3)\}_2] = (dadi)H_2 (N,N'-di-2-(2,6-diisopropylphenylamine)phenylglyoxaldi-imine)^{11,12,22,23}$ revealed divergent behavior dependent on the redox state of the ligand. When $(dadi^{4-})Ti^{IV}L$ (L = THF) was subjected to RX, alkylation occurred at the ene-diamide ligand backbone instead of an oxidative addition at the metal. In contrast, $(dadi^{2-})Ti^{IV}(=Y \text{ or } X_2)$ compounds were susceptible to nucleophilic attack at the ligand, which is now metrically assessed as a diimine. A crucial example of this reactivity is indicated in Figure 1, where thermolysis of $(dadi)TiCl_2$ induced internal attack by an amide on one backbone imine,

Received: May 30, 2023 Published: September 14, 2023





$$(\text{dadi}^2)\text{Tr}^{\text{IV}}\text{Cl}_2$$

$$|\text{pr-6,2}|$$

$$|\text{pr-6,$$

Figure 1. Discovery of (bida)TiCl₂ upon thermolysis of (dadi)TiCl₂ and aspects of the bida ligand that can contribute to reactivity via RNI, proton transfer, and lability.

followed by a 1,2-H-shift, to afford (bida)TiCl₂ (bida = N^1 -Ar- N^2 -((1-Ar-1-benzo[d]imidazol-2-yl)methyl)benzene-1,2-diamide; Ar = 2,6- i Pr-C₆H₃). 11

The present contribution focuses on initial studies of the bida ligand, which has several features worthy of examination in the context of chemical reactivity. Its aryl-diamide portion can reveal RNI (bidaⁿ, n = 0,1,2), t^{13-19} the ligand backbone has a methylene group that can potentially lead to reversible proton transfer, and the benzimidazole fragment may be hemilabile. Chromium was chosen as a target for investigation due to its multiple formal oxidation states and its potential for inter- and intraimido group transfer. Estimates of charge distribution in 1,2-diamide-aryl functionalities have been proposed by Wieghardt, providing some initial metric parameters for comparison. The studies support the fundamental conclusion that reliance on integer values to describe electronic states is often misleading.

RESULTS AND DISCUSSION

(bida)Na₂(THF)_n. Synthesis. While the initial preparation of bida-dianion occurred on titanium, the practicality of this method was obviously limited, so a "transition metal-free" rearrangement of (dadi)Na₂(THF)₄ was attempted with success. Thermolysis of blue (dadi)Na₂(THF)₄²² in THF for a day at 55 °C enabled the conversion to purple crystalline (bida)Na₂(THF)_n in 90% yield (eq 1). Its subsequent use required an ¹H NMR assay for the stoichiometry of THF present, as some loss to vacuum was often noted.

The ¹H NMR spectrum of (bida)Na₂(THF)_n in THF- d_8 showed a singlet at δ 4.25 and the requisite number of aromatic and isopropyl resonances, suggesting a plane of symmetry in solution, but crystallographic characterization of the crystalline dianion showed greater structural complexity.

Structure. Crystallization of (bida)Na2 from Et2O afforded the dimeric structure illustrated in Figure 2, the halves of which are related by a center of symmetry. The bida and one ether afford a highly distorted pseudoplanar core about Na1, with $/N1-Na1-Na2 = 67.05(4)^{\circ}, /N2-Na1-N4 = 69.53(4)^{\circ},$ $\angle N4-Na1-O1 = 91.33(4)^{\circ}$, and $\angle N1-Na1-O1 =$ 102.68(4)°. Angles from the apical O2 atom to the base range from 90.35(4) to 129.04(4)°. Pertinent metric parameters are given in Table 1, along with several other bida derivatives of chromium. The bond distances and angles are normal with a couple of exceptions. Sodium Na1 is asymmetrically bound to both arylamide nitrogens (2.5579(12) and 2.3580(11) Å), as is the second sodium (Na2; 2.4586(11) and 2.3592(11) Å), but the latter is also within a binding distance (2.80(13) ave) to the aryl-carbons of the 2,6-Pr₂-C₆H₄ group of the adjacent (bida)Na₂. Interestingly, one carbon-carbon bond distance (d(C009-C13) =1.4716(16) Å) greatly exceeds the remaining bonds within the aryl-diamide ring (1.402(12) Å), and these C-C bond lengths are longer than those of standard aromatics. As an internal standard, C-C bonds of the 2,6-iPr₂-C₆H₄ attached to the benzimidazole group average 1.392(11) Å, roughly the normal value. 45 Consequently, while the d(C-N) of 1.3660(16) and 1.3785(16) Å of the diamide might be construed as the limiting distance accorded a dianion, the distribution of electron density into the aromatic ring, as manifested by the elongated distances, provides some latitude in the interpreta-

(bida)CrCl(L) (1-L, L = THF, PMe₂Ph). Synthesis. Dianion (bida)Na₂(THF)_n was generated in situ from (dadi)-Na₂(THF)₄ in the presence of $CrCl_3(THF)_3^{46}$ for 12–16 h in THF at 23 °C to afford (bida)CrCl(THF) (1-THF) as

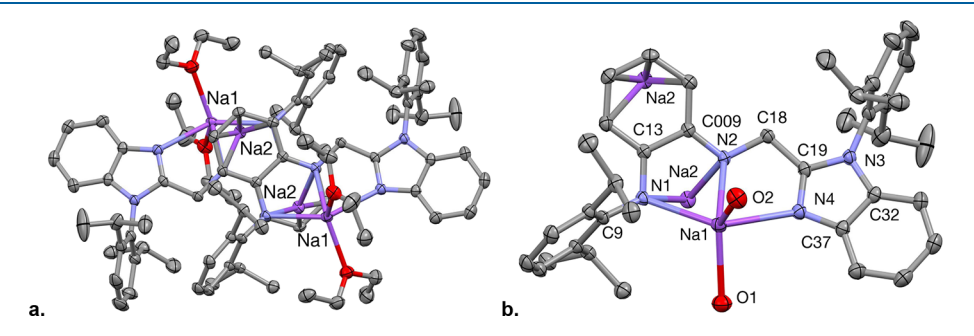


Figure 2. Molecular view of the dimer [(bida)Na₂(Et₂O)₂]₂ (a) and a truncated view of roughly half (b), which is related to its partner by inversion. Note that the atom labels are different from those of the chromium complexes, but the connectivities compared in Table 1 are correlated.

Table 1. Selected Comparative Distances (Å) and Angles (deg) in (bida)Na₂(THF)₄, (bida)CIV=NAr (4=NAr), (bida)Cr(X/L/Y),^a (bia)CrCl₂(THF) (8) and (bia)CrCl(CN(2,6-Me₂-C₆H₃)₂ (9) Compounds

	6	2.003(3)	1.966(3)	2.053(3)	1.426(4)	1.366(4)	1.422(4)	1.381(5)	1.351(4)	1.393(5)	1.375(4)	1.346(5)	2.3157(9)	2.072(3), 2.070(3)	80.90(12)	160.28(12)	79.41(13)	100.02(8), 93.93(3)	178.50(7), 84.22(3)	99.69(9), 86.04(3)	96.73(12), 91.42(12)	88.44(12), 85.20(12)	81.93(12), 87.77(11)	92.63(10), 93.58(10)	112.2(3)
	œ	2.0127(11)	1.9963(12)	2.0771(12)	1.4307(18)	1.3544(18)	1.433(2)	1.3751(18)	1.3314(19)	1.4550(19)	1.3586(18)	1.3268(18)	2.3106(3), 2.3377(3)	2.0463(10)	81.47(5)	161.40(5)	80.03(5)	93.16(3)	91.84(3)	85.63(3)	99.30(4)	176.62(4)	99.28(4)	91.41(3), 92.43(3)	111.92(12)
ipr-6.2 N1 - Cr - N4 XIL XIL X	7	1.9406(13)	1.9354(14)	2.0939(13)	1.430(2)	1.383(2)	1.425(2)	1.371(2)	1.446(2)	1.493(2)	1.358(2)	1.325(2)	2.0906(14)	2.0411(14)	80.57(6)	150.25(6)	78.56(6)	98.22(6)	175.72(6)	104.02(6)	116.36(6)	115.04(6)	91.75(6)	61.76(6)	104.99(13)
	6 = NAr	1.9671(12)	1.9259(11)	2.0510(11)	1.4480(17)	1.3857(18)	1.4212(19)	1.3782(17)	1.4533(17)	1.4867(19)	1.3586(17)	1.3194(17)	2.0749(14)	1.6689(11)	80.72(5)	158.28(5)	77.56(5)	99.66(5)	115.37(5)	89.69(5)	101.93(5)	142.99(5)	95.45(5)	100.71(6)	104.28(10)
in-6.2 (M)	5 = NAr	1.9566(11)	1.9381(11)	2.0533(11)	1.4350(16)	1.3814(17)	1.4201(18)	1.3794(16)	1.4395(16)	1.4836(18)	1.3561(16)	1.3184(17)	2.0521(14)	1.6734(12)	79.96(5)	157.71(5)	77.84(4)	99.46(5)	108.61(6)	89.49(5)	102.33(5)	147.36(5)	95.35(5)	103.14(6)	104.85(10)
Pr-6/2 P	4 = NAr	1.9560(16)	2.0071(15)	2.0889(16)	1.442(2)	1.385(2)	1.420(2)	1.380(2)	1.428(2)	1.480(3)	1.355(2)	1.321(2)	2.2352(6)	1.6793(16)	78.55(6)	152.82(6)	75.63(6)	104.99(5)	112.15(2)	92.57(5)	100.15(7)	135.54(7)	92.43(7)	111.02(6)	105.39(15)
	3 = NAd	1.966(3)	1.902(3)	2.050(3)	1.434(5)	1.364(5)	1.413(6)	1.380(5)	1.441(5)	1.494(6)	1.355(5)	1.309(5)	2.2659(11)	1.651(4)	80.26(14)	151.38(14)	78.35(13)	92.85(9)	134.69(11)	88.87(9)	109.94(15)	111.36(16)	95.50(14)	113.04(14)	104.5(3)
	2-Nph	1.9814(18), 1.9808(19)	1.9306(18), 1.9317(18)	2.0970(18), $2.1020(18)$	1.422(3), 1.429(3)	1.384(3), 1.389(3)	1.429(3), 1.431(3)	1.378(3), 1.372(3)	1.440(3), 1.437(3)	1.493(3), 1.483(3)	1.360(3), 1.354(3)	1.330(3), 1.330(3)	2.092(2), 2.085(2)	2.1118(15), 2.1141(15)	80.93(8), 80.62(8)	155.06(7), 156.32(7)	78.74(7), 78.81(7)	108.67(8), 103.80(9)	114.59(8), 113.53(8)	92.92(8), 95.11(8)	98.18(7), 97.77(7)	158.14(7), 157.98(7)	95.38(7), 96.91(8)	86.54(7), 88.27(8)	105.31(16),
iPr-6.2 (bida)	2-Me	1.983(2)	1.923(2)	2.100(2)	1.425(3)	1.394(3)	1.427(3)	1.375(3)	1.422(3)	1.490(3)	1.356(3)	1.320(3)	2.076(3)	2.092(2)	80.73(9)	156.08(8)	79.42(9)	108.87(11)	106.85(12)	89.64(11)	99.30(9)	159.11(10)	94.57(9)	93.00(13)	105.3(2)
<u>ċ</u>	$1-PMe_2Ph$	1.9672(11)	1.9357(11)	2.1005(11)	1.4330(17)	1.3842(17)	1.4247(18)	1.3710(17)	1.4484(16)	1.4887(18)	1.3574(17)	1.3240(17)	2.3198(4)	2.4585(4)	80.14(5)	151.43(5)	78.52(5)	97.54(3)	159.69(4)	95.92(3)	110.79(4)	106.79(4)	93.50(4)	92.954(14)	104.92(10)
	$(bida)Na_2$	2.5579(12)	2.3580(11)	2.5239(12)	1.4150(15)	1.3785(16)	1.4716(16)	1.3660(16)	1.4419(15)	1.4969(18)	1.3825(16)	1.3186(17)		2.4372(12), 2.4317(11)											
	d/angle	M-N1	M-N2	M-N4	N1-C9	N1-C13	C13-C18	N2-C18	N2-C19	C19-C20	C20-N3	C20-N4	M-X	M-L/Y	N1MN2	N1MN4	N2MN4	XMN1	XMN2	XMN4	N1ML/Y	N2ML/Y	N4ML/Y	XML/Y	N2C19C20

^aFor the (bida)Cr derivatives, comparable core distances (Å) and angles (deg) average: CrN1, 1.972(10); CrN2, 1.927(12); CrN4, 2.079(26); N1-Cr-N2, 80.48(36); N1-Cr-N4, 155.2(28); N2-Cr-N4, 78.46(62). For the (bida)Cr and V derivatives, comparable core distances (Å) and angles (deg) average: N1C9, 1.434(8); N1C13, 1.383(9); C13C18, 1.423(6); N2C18, 1.377(4); N2C19, 1.439(10); C19C20, 1.487(5); C20N4, 1.321(7); N2-C19-C20, 105.0(4).

Scheme 1. Syntheses of (bida)CrCl(THF) (1-THF) and Derivative (bida)CrCl(PMe,Ph) (1-PMe,Ph)

$$\begin{array}{c} \text{(Idadi)Na}_2 \\ \text{in situ} \\ \text{(bida)Na}_2 \\ \\ \text{23°C} \\ \text{12-16 h} \\ \end{array} \begin{array}{c} \text{CrCl}_3(\text{THF})_3 \\ \text{N} \\ \text{Cr} \\ \text{THF} \\ \text{Cl} \\ \text{1-THF} \\ \text{97\%} \\ \mu_{\text{eff}} = 3.4 \ \mu_{\text{B}} \\ \end{array} \begin{array}{c} \text{2,6-iPr} \\ \text{PMe}_2\text{Ph} \\ \text{23°C, 30 min} \\ \text{L} = \text{PMe}_2\text{Ph} \\ \text{23°C, 30 min} \\ \text{Meff} = 3.8 \ \mu_{\text{B}} \\ \text{Meff} = 3.8 \ \mu_{\text{B}} \\ \end{array}$$

green crystals in excellent yield (97%, Scheme 1). Evans' method⁴⁷ measurements were consistent with a standard Cr(III), S=3/2 core, as $\mu_{\rm eff}=3.4(1)$ $\mu_{\rm B}$, a value slightly attenuated from the spin-only number of 3.87 $\mu_{\rm B}$ due to spin-orbit coupling (SOC).⁴⁸ Assignment of its ¹H NMR spectrum proved difficult; hence, single crystal X-ray diffraction (XRD) methods were employed, but a satisfactory structural solution was hampered by twinning/disorder effects. The addition of PMe₂Ph to 1-THF converted it to a phosphine adduct, (bida)CrCl(PMe₂Ph) (1-PMe₂Ph), which was harvested as dark red crystals in 93% yield. A single ³¹P NMR spectral resonance at $\delta - 46.16$ ($\nu_{1/2} = 740$ Hz) was observed, and Evans' method measurements provided a $\mu_{\rm eff}$ of 3.8(1) $\mu_{\rm B}$, a reasonable value for a conventional S=3/2 Cr(III) center with minimal contributions from SOC.⁴⁸

Structure of (bida)CrCl(PMe₂Ph) (1-PMe₂Ph). A single crystal X-ray crystallographic study performed on (bida)CrCl-(PMe₂Ph) (1-PMe₂Ph) afforded the molecular view in Figure 3. Pertinent comparable metric parameters are provided in

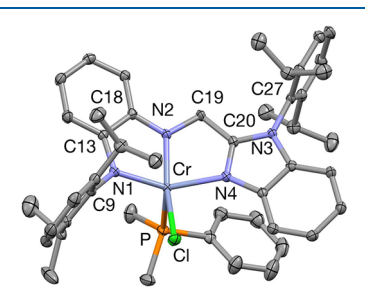


Figure 3. Molecular view of (bida)CrCl(PMe₂Ph) (1-PMe₂Ph); selected metric parameters are given in Table 1.

Table 1. 1-PMe₂Ph is a highly distorted square pyramid (Addison ⁴⁹ parameter $\tau = 0.14$) with the phosphine occupying the apical position and basal angles that reflect the respective "bites" of the bida ligand: $\angle N1-Cr-N2 = 80.14(5)^{\circ}$, $\angle N1-Cr-N4 = 151.43(5)^{\circ}$, $\angle N2-Cr-N4 = 78.92(5)^{\circ}$, $\angle N1-Cr-C1 = 97.54(3)^{\circ}$, $\angle N2-Cr-C1 = 159.69(4)^{\circ}$, $\angle N4-Cr-C1 = 95.92(3)^{\circ}$. The apical P to basal atom angles range from $92.954(14)^{\circ}$ to $110.79(4)^{\circ}$. The d(Cr-N1) of

1.9672(11) Å is slightly longer than d(Cr-N2) = 1.9357(11) Å, presumably due to greater steric influences on the former, and conformational restrictions on the pincer that impose a shorter than normal Cr contact with N2. Both amides are considerably shorter than the bond distance of 2.1005(11) Å pertaining to the neutral donor benzimidazole (Cr-N4). The remaining distances are normal and consistent with C19 as a methylene group. ⁴⁵

Wieghardt et al. have assessed the charges on o-1,2-diamide/diimine-benzo (o-C₆H₄(NH)₂) ligands and have settled on d(CN) and d(CC) values to be roughly as follows: charge = 0 (oxidized), d(CN) = 1.30 Å, d(CC) = 1.45 Å; charge = -1 (o-diiminobenzosemiquinonate), d(CN) = 1.35 Å, d(CC) = 1.42 Å; - 2, (benzodiamide), d(CN) = 1.39 Å, d(CC) = 1.40 Å.^{41-44,50} Equations of charge derived from this analysis (c = {d(CN)-1.3017}/(-0.045); c = {d(CC) - 1.4483}/(0.0250)) afforded bida $^{n-}$ as n = -1.7 from the d(CN) values and n = -1.0 from the d(CC) numbers. In bida, the position of one amide in the interior of the pincer is likely to distinguish the metrics from o-C₆H₄(NH)₂ ligands based on the constraints of tridentate ligation. Although fractional charges can lead to metrical oxidation states as proposed by Brown, 51 and these may be a true indication of electron density, $^{52-55}$ equations of charge specific to bida were sought.

Using N1–C9 as a reference distance, $[(bida)Na_2(Et_2O)_2]_2$ provided an additional standard, with the caveats discussed above. Checking other ligands that possess the dichotomous diamide/diamine functionality, modified equations of charge were determined to be roughly (c = d(CN)ave -1.32 Å)/ (-0.055)) and (c = d(CC) - 1.45 Å)/(0.025)). A charge calculation of bida in (bida)CrCl(PMe₂Ph) (1-PMe₂Ph) from this equation afforded a (bida)ⁿ as n = -1.1 (from d(CN)) or n = -1.0 (from d(CC)), hence we assign a configuration of (bida⁻¹)[↓]Cr^{↑↑↑↑}Cl(PMe₂Ph), i.e., high spin Cr(II) antiferromagnetically coupled to the diamide radical anion, for a total spin of $S_T = 3/2$. Since there are no direct models of bida and the use of Wieghardt's charges provides ambiguity (c = -1.7, – 1.0), a conventional Cr(III) ground state, i.e., (bida⁻²)Cr^{↑↑↑}Cl-(PMe₂Ph), remains in consideration, as calculations (vide infra) also accord it as having at least equal merit.

Scheme 2. Metathetical Routes to (bida)Cr Alkyl Complexes

(bida)CrR Complexes. Syntheses. Metatheses of (bida)CrCl(THF) (1-THF) were conducted with solid alkyllithiums in diethyl ether at 23 °C for ~16 h, as illustrated in Scheme 2. The smallest alkyllithium, MeLi, produced green (bida)CrMe-(THF) (2-Me) in 62% yield upon crystallization from Et₂O, despite the fact that only THF present was the initial adduct on the chloride, 1-THF. Evans method⁴⁷ analysis afforded a $\mu_{\rm eff}$ of 3.6(1) $\mu_{\rm B}$, a value consistent with the expected S=3/2 core, somewhat attenuated by SOC effects, and this was corroborated by the EPR spectrum of (2-Me) shown in Figure 4. Neophyllithium ((Nph)Li) was used to make light-green

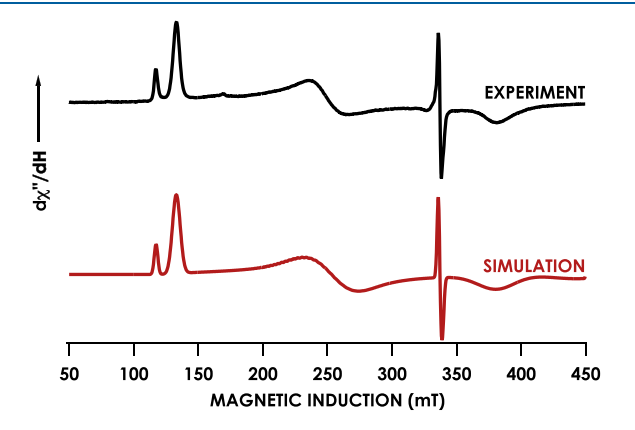


Figure 4. CW EPR spectrum of (bida) CrMe(THF) (2-Me) observed in toluene at 100 K (black) and the simulated spectrum (red). Fitting the spectrum shows the primary component (>99%) as an S=3/2 system with $g_x=1.857$, $g_y=2.015$, and $g_z=1.958$; the secondary component (<1%) is a S=1/2 system with $g_x=1.879$, $g_y=1.78$, and $g_z=1.962$.

microcrystalline (bida)CrCH₂CMe₂Ph(THF) (2-Nph), which was isolated in 76% yield and has a $\mu_{\rm eff}$ of 3.4(1) $\mu_{\rm B}$ consistent with an S=3/2 core.

Structures of (bida)CrR(THF) (2-R; R = Me, Nph). With an Addison⁴⁹ value of $\tau = 0.05$, (bida)CrMe(THF) (2-Me), shown in Figure 5, is a pseudosquare pyramid due to its

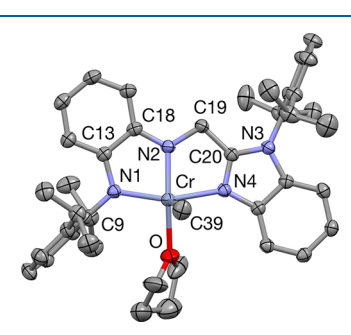


Figure 5. Molecular view of (bida)CrMe(THF) (2-Me); selected metric parameters of 2-Me and (bida)Cr(neophyl)(THF) (2-Nph) are given in Table 1. A view of structurally related 2-Nph is included in the Supporting Information.

relatively flat base compared to the other bida derivatives. Acute basal angles correspond to the bite angles of the diamide and amide-benzimidazole sides of bida, and angles to the THF oxygen compensate: $\[N1-Cr-N2 = 80.73(9)^\circ, \] \[N1-Cr-N4 = 156.08(8)^\circ, \] \[N2-Cr-N4 = 79.42(9)^\circ, \] \[N1-Cr-O = 99.30(9)^\circ, \] \[N2-Cr-O = 159.11(10)^\circ, \] and \] \[N4-Cr-O = 94.57(9)^\circ.$ The methyl group, as the greatest *trans*-influence ligand and slightly smaller than THF, occupies the apical

position, with C–Cr–N/O angles ranging from 89.64(11)° to 108.87(11)° with respect to the basal positions. The d(Cr–C) distance of 2.076(3) Å is relatively short, ⁵⁶ in accordance with its apical position, and the remaining core distances (CrN1, 1.983(2) Å; CrN2, 1.923(2) Å; CrN4, 2.100(2) Å), including all C–N and C–C bond lengths of the chelate, are within 2σ of the average of the six (bida)Cr(R/X)(L/=NR') structures in Table 1.

Using the aforementioned modified equations of charge $(d(CN)ave-1.32\ \text{Å})/(-0.055)$ and $(d(CC)-1.45\ \text{Å})/(0.025)$, values of -1.1 (from d(CN)) and -0.9 (from d(CC)) for bida lead to the conclusion that bida is best construed as a monoanion. A configuration of $(bida^{-1})^{\downarrow}Cr^{\uparrow\uparrow\uparrow\uparrow}Me(THF)$, i.e., high spin Cr(II) antiferromagnetically coupled to the diamide radical anion, is assessed to the complex, yielding a total spin of $S_T=3/2$, but once again, the Cr(III) ground state, i.e., $(bida^{-2})Cr^{\uparrow\uparrow\uparrow}Me(THF)$ must be kept in consideration.

Core metric parameters of (bida)Cr(Nph)(THF) (2-Nph), listed in Table 1, are close to those of (bida)CrMe(THF) (2-Me), rendering an analogous ground state configuration of (bida $^{-1}$) $^{\downarrow}$ Cr $^{\uparrow\uparrow\uparrow\uparrow}$ Nph(THF), where high spin Cr(II) is AF-coupled to the diamide radical anion, for a total spin of $S_T = 3/2$, hedged by the alternative (bida $^{-2}$)Cr $^{\uparrow\uparrow\uparrow}$ Nph(THF) configuration. Charge calculations from the empirical equation of charge above afford values of -1.1 (from d(CN)) and -0.8 (from d(CC)) (Scheme 3).

Scheme 3. Syntheses of Formally Cr(V) (bida)ClCr=NR (R = Ad, 3=NAd; 2,6- ${}^{i}Pr_{2}C_{6}H_{3}$, 3=Ar) via Azide Addition to (bida)CrCl(THF) (1-THF), and the Salt Metathesis Route to V(V) (bida)ClV=NAr (4=NAr)

(bida)CICr=NR and (bida)CIV=NAr Complexes. Syntheses. The nature of the geometries and ground states of (bida)LCrCl (L = THF, 1-THF; PMe₂Ph, 1-PMe₂Ph) and (bida)CrR(THF) (2-R; R = Me, Nph) prompted oxidation studies. Common azides⁵⁷ were chosen as substrates: adamantyl azide (AdN₃) as a precursor to an electron-donating nitrene/imido, and 2,6- i Pr₂C₆H₃N₃ as a generator for a corresponding modestly electron-withdrawing fragment.

Treatment of (bida)ClCr(THF) (1-THF) with AdN₃ or 2.6^{-i} Pr₂C₆H₃N₃ (ArN₃) in benzene at room temperature overnight yielded dark green crystalline material upon workup in hexanes. The adamantyl derivative (bida)ClCr=NAd (3= NAd) was isolated in 96% yield, while the diisopropylphenylmido complex (bida)ClCr=NAr (3=NAr) was collected in 61% yield. Evans' method⁴⁷ measurements on 3=NAd produced a $\mu_{\rm eff}$ of 2.4(1) $\mu_{\rm B}$, while the corresponding value for 3=NAr was 2.3(1) $\mu_{\rm B}$. This is an atypical value for a "Cr(V)"

 d^1 species, whose values are usually near the spin-only number of 1.73 μ_B , again hinting at an unusual electronic configuration. As shown in Figure 6, the EPR spectrum of 3—NAr was a rather nondescript S = 1/2 signal at $g_{iso} = 1.99$.

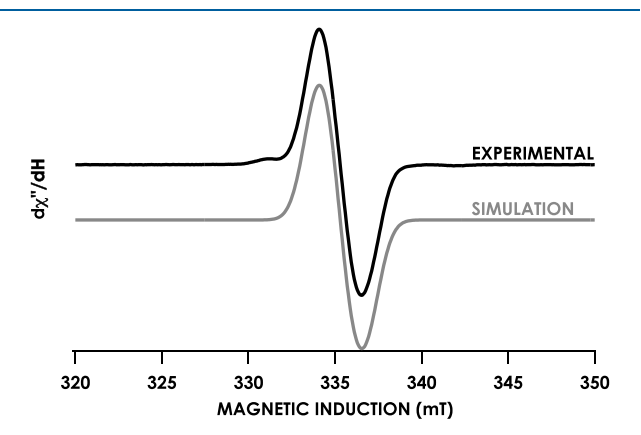


Figure 6. CW EPR spectrum of (bida)ClCr=NAr (3=NAr, Ar = $2,6^{-i}$ Pr₂C₆H₃) observed in 2-Me-THF at 110 K (black) and its simulated spectrum (gray), which afforded a fit of the S=1/2 system with $g_x=1.99, g_y=1.99,$ and $g_z=1.98.$

Assignments of ¹H NMR spectra were complicated due to paramagnetic broadening, and several species were completely NMR silent. To provide some information, a diamagnetic reference was sought, and the addition of (dadi)Na₂ (in situ rearranged from (bida)Na₂) to ArN = VCl₃ afforded brown crystalline (bida)CIV=NAr (4=NAr) in a decent yield (48%). The asymmetric molecule served to reveal the multiple isopropyl groups, aromatics, and the unique methylene doublet of doublets at δ 4.62 and 4.98 with J = 29.6 Hz.

Structures of (bida)CICr=NAd (3= NAd) and (bida)-CIV=NAr (4=NAr). A molecular view of (bida)CICr=NAd (3=NAd) is shown in Figure 7, and selected interatomic

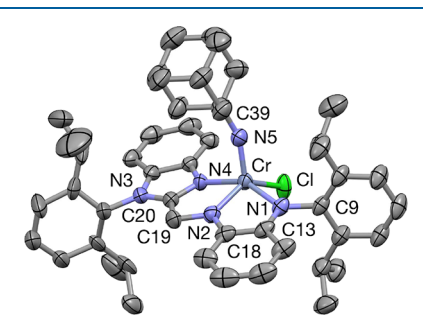


Figure 7. Molecular view of (bida)ClCr=NAd (3=NAd); selected metric parameters for 3=NAd and (bida)ClV=NAd (4=NAr) are given in Table 1.

distances and angles are provided in Table 1. Imide 3—NAd is unusual in that it crystallized in the trigonal system (space group R3), and significant disorder was evident in the 2,6-diisopropylphenyl group attached to the benzimidazole. With the disorder modeled, the structure solution revealed a highly disordered square pyramid ($\tau = 0.28$), with the imido functionality in its pseudoapical position possessing a d(CrN5) of 1.651(4) Å and a \angle Cr-N5-C39 angle of 156.3(3)°. The imido nitrogen (N5) is bent at 109.94(15)°, 111.36(16)°, and 95.50(14)° with respect to the N1, N2, and N4 nitrogens of bida and 113.04(14)° to the chloride. In modest contrast, the

chloride (Cl) angles to N1, N2, and N4 are $92.85(9)^{\circ}$, $134.69(11)^{\circ}$, and $88.87(9)^{\circ}$, respectively. The formal oxidation of "Cr(III)" to "Cr(V)" failed to elicit any substantial changes in the core or bida distances, as every pertinent metric was within 2σ of the average of the other five five-coordinate (bida) Cr structures shown in Table 1.

With magnetic moments suggestive of an atypical $S_{\rm T}=1/2$ ground state, a classical description of 3—NAd such as (bida²-)ClCr³-NAd is questionable. If bida is truly monoanionic, as implied by empirically generated charges of -1.1 (from d(CN)) and -1.5 (from d(CC)), at least one other ligand must possess unpaired spin density. Imidyl character has been characterized in a few, sterically protected Cr imido complexes, $^{36-38}$ and with this precedent, an alternative electronic ground state would be (bida $^{-1}$) $^{\downarrow}$ (Cl $^{1-}$)-Cr $^{\uparrow\uparrow\uparrow}$ (NAd $^{-1}$) $^{\downarrow}$, requiring two AF-coupled pairs of electrons. If bida is rendered a dianion, a "Cr(IV)" description, i.e., (bida $^{-2}$)(Cl $^{1-}$)Cr $^{\uparrow\uparrow}$ (NAd $^{-1}$) $^{\downarrow}$, could still implicate significant imidyl character.

Diamagnetic (bida)ClV=NAr (4=NAr), has a structure much closer to a trigonal bipyramid ($\tau=0.68$)⁴⁹ than 3=NAd, but virtually all the metrical data (see Table 1) other than core angles mirror the chromium species. Even the d(VN) of 1.6793(16) Å^{58,59} is essentially the same as 3=NAd once the differences in covalent radii (\sim 0.04 Å) are considered.

(bida)R'Cr=NR Complexes. Syntheses. In addressing the possibility of unusual insertion processes of alkyl/imido species, 60-64 alkyl derivatives of (bida) ClCr=NR (3=NR, R = Ad, Ar) were sought. The addition of MeLi or neophyllithium to 3=NR in diethyl ether at 23 °C for 12-16 h resulted in reasonable yields of the four possible alkyl/imido complexes, (bida)R'Cr=NR (R'=Me, R=Ad(70%), Ar (74%), 5=NR; R' = CH₂CMe₂Ph (Nph), R = Ad (60%), Ar (65%), 6=NR; Scheme 4). Each complex was a subtle variation of brown- or wine-red, and each possessed a $\mu_{\rm eff}$ of 2.3(1)-2.4(1), in line with the precursor chloride complexes, according to Evans' method measurements. Again, d¹ "Cr(V)" cores are expected to possess μ_{eff} values near or below the spin-only value of 1.73 $\mu_{\rm B}$, yet the observed values for the class of (bida)(R/X)Cr=NR' complexes are consistently in a regime well above μ_{SO} . It seems likely that such observations are a sign of unconventional ground states.

Nitrene transfer from RN₃ to (bida)(THF)CrR (R = Me, 2-Me; CH₂CMe₂Ph (2-Nph)) was considered an alternative route to imidoalkyls, but when 2-Nph was subjected to ArN₃ (Ar = 2,6- i Pr₂-C₆H₃), nitrene transfer did not occur. Instead, an unusual migratory insertion of ArN₃ into the Cr–C bond occurred without any N₂ loss to afford the crystalline red (bida)Cr(κ^2 -N,N-ArN₃neophyl) (7) in 83% yield. From Evans' method measurements, a value of $\mu_{\rm eff}$ of 3.1 i $\mu_{\rm B}$ was obtained, consistent with an $S_{\rm T}$ = 3/2 center significantly attenuated by spin-orbit effects. It may be that γ -coordination of ArN=N=N must occur prior to N₂ loss, $^{36,65-67}$ and if the adjacent position to azide binding is a chloride, reversible α - to γ -coordination can occur. If an alkyl is present, an alternative, swifter path to insertion is present and N₂ loss is averted.

Structures of (bida)R'Cr=NAr (R' = Me, 5=NAr; neophyl, 6=NAr) and (bida)Cr(κ^2 -N,N-ArN₃Nph) (7). Figure 8 reveals a molecular view of (bida)(neophyl)Cr=NAr (6= NAr, τ = 0.25), 49 which is a highly distorted square pyramid, presumably due to greater steric constraints imposed by the pseudoapical neophyl ligand. The d(Cr-C) is 2.0749(14) Å,

Scheme 4. Syntheses of Formally Cr(V) Imido $(Ar = 2,6^{-i}Pr_2C_6H_3)$ Derivatives (bida)R'Cr=NR (R' = Me, R = Ad, Ar, 5=NR; R' = Neophyl, R = Ad, Ar, 6=NR) and the Azide Insertion Product (bida)Cr(κ^2 -N,N-ArN₃neophyl) (7)

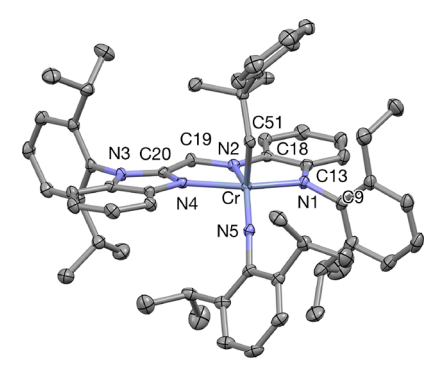


Figure 8. Molecular view of the alkyl imide (bida)(PhMe₂CH₂)Cr=NAr (6=NAr, $\tau = 0.25$); selected metric parameters for (bida)-MeCr=NAr (5=NAr, $\tau = 0.17$; see the Supporting Information) and 6=NAr are given in Table 1.

slightly longer than that of 5=NAr (2.0521(14) Å), likely due to sterics and the modestly stronger BDE expected for Me. The metal imido distances, 1.6734(12) Å for 5=NAr and 1.6689(11) Å for 6=NAr, are essentially the same and only \sim 0.02 Å longer than the d(CrN) of 3=NAd, which can be rationalized as resulting from the chloride having a slightly more electrophilic metal center.

Bida core values listed for both alkylimides in Table 1 reveal striking similarities not only to (bida)ClCr=NAd (3=NAd) and (bida)ClV=NAr (4=NAr) but also to the formally "Cr(III)" five-coordinate complexes. Consequently, all derivatives have average bida charges of -1.08(2) (from d(CN)) or -1.06(22) (from d(CC)) if the above equation of charge is utilized. Switching to Wieghardt's assessment of o-diaminobenzene complexes changes the charges to -1.73(2) and -1.00(22), presenting greater ambiguity yet still metrically presenting the bida ligand as being *effectively* monoanionic. As commented on below, calculational support for this assessment is ambiguous, as nonintegral values are assessed in the representative complexes.

Structure of $(\overline{bida})Cr(\kappa^2-N,N-ArN_3Nph)$ (7). Shown in Figure 9 is a molecular view of $(\overline{bida})Cr(\kappa^2-N,N-ArN_3Nph)$ (7), the migratory insertion product generated from $(\overline{bida})-Cr(Nph)(THF)$ (2-Nph) and 2,6- iPr_2N_3 (ArN₃). Core

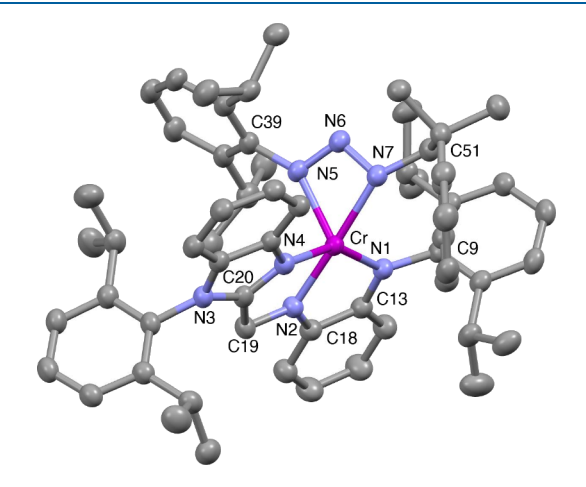


Figure 9. Molecular view of azide insertion product (bida) Cr(κ^2 -N,N-ArN₃Nph) (7). Core metric values are given in Table 1. Other selected interatomic distances (Å) and angles (deg): N5–N6, 1.322(2); N6–N7, 1.316(2); N5–C39, 1.419(2); N7–C51, 1.462(2); Cr–N5–N6, 96.58(9); N5–N6–N7, 107.01(13); N6–N5–C39, 117.69(14); N6–N7–C51, 113.74(14); Cr–N5–N6, 96.58(9); Cr–N7–N6, 94.47(10); Cr–N5–C39, 145.47(12); Cr–N7–C51, 148.63.

distances and angles pertaining to the bida ligand are essentially the same as the prior examples containing this chelate and are given in Table 1, while parameters featuring the κ^2 -N,N-ArN₃Nph ligand can be found in the footnote of Figure 9. The unusual κ^2 -N,N-ArN₃Nph ligand^{67–70} takes up one position (N7(Nph)) in a distorted square plane whose angles sum to 361.37°, and another pseudo axial position (N5(Ar)) that results in a bite angle of 61.77(6)°. The 107.01(13)° N5–N6–N7 angle, and N–N distances of 1.322(2) and 1.316(2) Å suggest that κ^2 -N,N-ArN₃Nph binds as a delocalized triazaallyl anion,⁴⁵ with a slightly shorter Cr–N-(axial) distance of 2.0411(14) Å than its pseudo basal partner (d(Cr–N7) = 2.0906(14) Å). Given the triazaallyls bite, angles of the apical N5 to N1, N2, and N4 are highly varied at 116.36°, 115.04°, and 91.75(6)°, respectively.

Bida to Bia Backbone. *Oxidations.* Oxidation of (bida)-CrCl(THF) (1-THF) was also conducted with N-chlorosucci-

Scheme 5. Reactions Involving Hydrogen Loss from (bida) To Afford (bia) $CrCl_2(THF)$ (8) and (bia) $ClCr(CNAr')_2$ (9, $Ar' = 2,6-Me_2C_6H_3$)

$$\begin{array}{c} \text{1.THF} \\ \text{2.6-Pr} \\ \text{3=NAd} \\ \text{$$

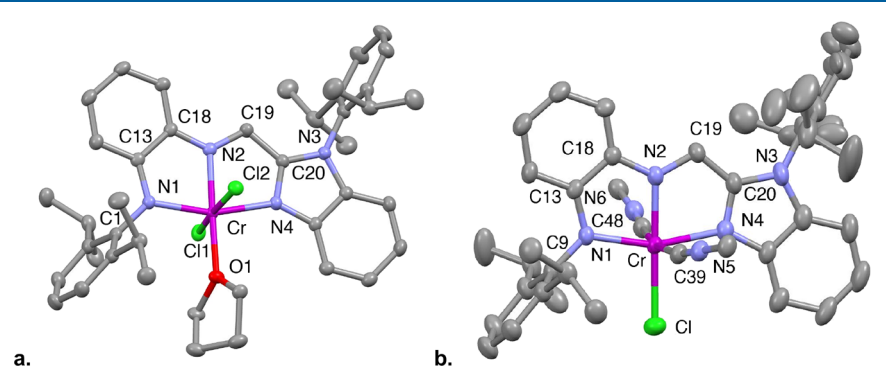


Figure 10. Molecular views of (bia) $CrCl_2(THF)$ (8, a) and (bia) $ClCr(CNAr')_2$ (9, Ar' = 2,6- $Me_2C_6H_3$, b, only the ipso carbons of the 2,6- $Me_2C_6H_3$ groups are shown).

nimide (NCS), producing the dichloride (bia)CrCl₂(THF) (8, biaⁿ = benzimidazole-imine-amide), as shown in Scheme 5. While the target was a Cr(IV) chloride, oxidation of bida to an amide-diimine occurred instead, likely proceeding via Cl-atom abstraction from NCS, and H atom abstraction by succinimide radical on the methylene group in the ligand backbone. Whether this occurs in a bimolecular fashion or by radical chain is unknown, but 8 was produced in 70% yield and possesses a $\mu_{\rm eff}$ of 3.6(1) $\mu_{\rm B}$, consistent with the expected S=3/2 center ligated by a monoamide.

A more unusual oxidation occurs when the adamantyl imide (bida)ClCr=NAd (3=NAd) is exposed to excess 2,6dimethylphenylisocyanide $(2,6-Me_2C_6H_3NC = Ar'NC)$. While imide transfer to Ar'NC - and catalytic carbodiimide catalysis²⁷ was targeted - HAT from bida was observed concomitant with imide loss, and (bia)ClCr(CNAr') (9) was isolated as dark red crystals (51%). The formulation as Cr(IV) was dictated by the $\mu_{\rm eff}$ of 2.6(1) $\mu_{\rm B}$, and metrics were more consistent with the triamide form of the bia ligand. Its IR spectrum manifests two $\nu(\text{CN})$ stretches at 2145 and 2088 cm⁻¹, consistent with the two isocyanides. ¹H and ¹³C NMR spectra of residual material obtained upon removal of volatiles from the filtrate revealed adamantyl resonances that did not correspond to AdNH2, but no aromatic signals. Mass spectral assessment of the solution by DART revealed only AdNH2, which is a plausible degradation product. It is conceivable that initial coordination by Ar'NC enables the AdN=Cr to undergo HAT to AdNH-Cr, leading to unknown products containing this fragment, perhaps (AdNH)₂. With the modest

yield, there are a considerable number of speculative paths, including bimolecular ones, that could be invoked to afford 9.

Structure of (bia)CrCl₂(THF) (8). A molecular view of dichloride (bia)CrCl₂(THF) (8) is given in Figure 10a., and pertinent metrics are given in Table 1. The core is a fairly regular octahedron, despite the constraints of the bia bite angles $(/N1-Cr-N2 = 81.47(5)^{\circ}, /N2-Cr-N4 =$ 80.03(5)°), and the remaining angles between adjacent atoms about Cr average 91.72(52)°. Core distances are slightly longer than the lower coordinate derivatives, as d(CrN1) is ~0.04 longer at 2.0127(11) Å, and d(CrN2) is \sim 0.06 Å longer at 1.9963(12) Å, although the benzimidazole nitrogen is roughly the same at 2.0771(12) Å. The d(CrCl) are 2.3106(3) and 2.3377(3) Å, about the same as that in 1-PMe₂Ph. The key change in the bida ligand involves its loss of a H atom, and change in the N2-C19-C12 angle from an average of 105.0(4)° to 111.92(12)°, consistent with its change from an sp³- to an sp²-carbon, albeit one constrained within the pincer. The d(C19C20) of 1.4550(19) Å is \sim 0.03 Å shorter,⁴⁵ commensurate with the change in hybridization.

Structure of (bia)ClCr(CNAr')₂ (9). Illustrated in Figure 10b is a molecular view of (bia)ClCr(CNAr')₂ (9, Ar' = 2,6-Me₂C₆H₃) with only the ipso carbons of the 2,6-dimethylphenyl group shown for clarity. Metric observations pertaining to 8 are similar to those features on 9 with some critical exceptions. The hybridization change from the methylene in bida to an =CH- in bia is again noted as the N2-C19-C12 angle differs from the average of 105.0(4)° to 112.2(3)°, but the accompanying d(C19C20) is 1.393(5) Å, which is \sim 0.09 Å

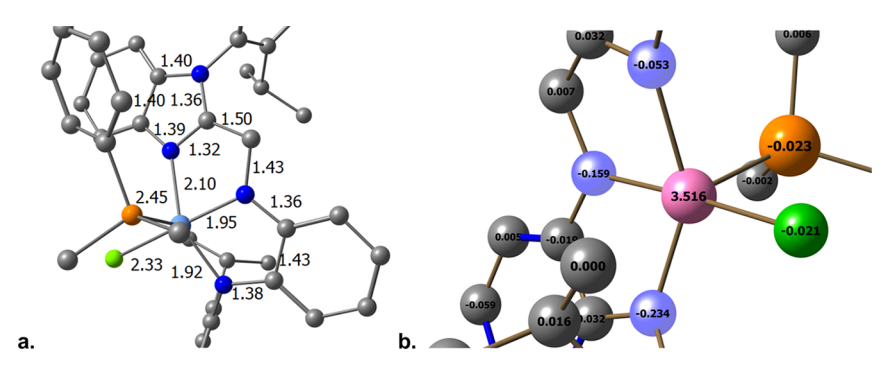


Figure 11. Calculated geometry (a, ONIOM(M06/6-31G(d):UFF), $2,6^{-i}$ Pr₂C₆H₃ groups in the MM partition, remainder in the QM region), and Mulliken spin densities (in e⁻) (b) of (bida)CrCl(PMe₂Ph) (1-PMe₂Ph) highlight atoms of consequence that indicate a plausible mix of Cr(II) and Cr(III) states.

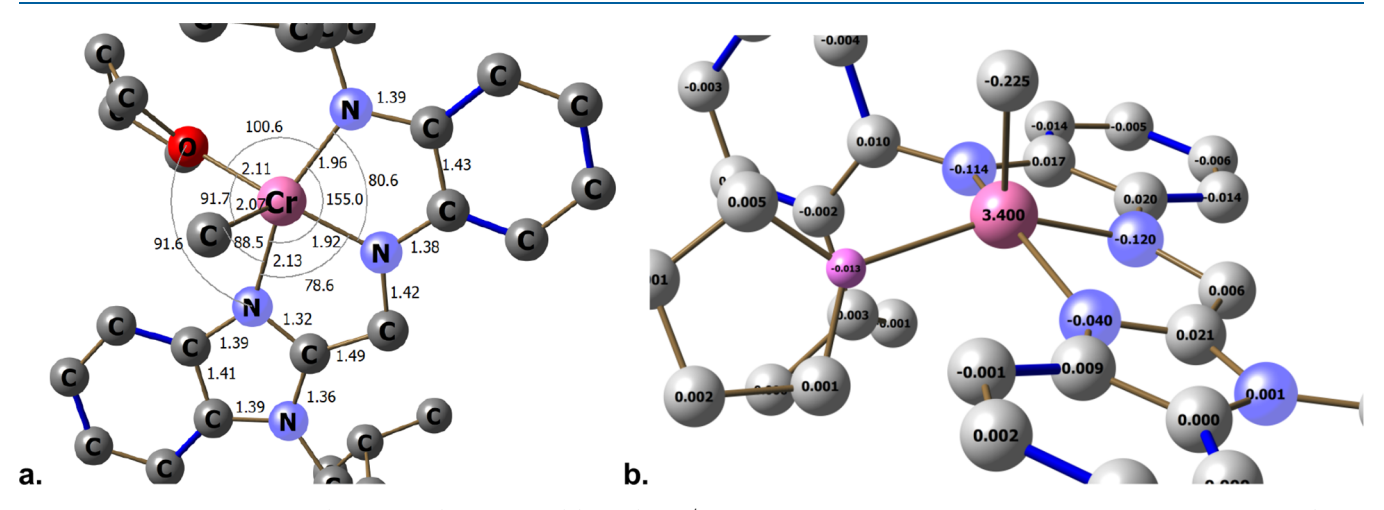


Figure 12. Calculated geometry (a, ONIOM(M06/6-31G(d):UFF), $2,6^{-i}$ Pr₂C₆H₃ groups in the MM partition, remainder in the QM region) and Mulliken spin densities (in e⁻) (b) of (bida)CrMe(THF) (2-Me) highlight atoms of consequence that indicate a plausible mix of Cr(II) and Cr(III) states.

shorter than the bida average. Consequently, while bia is best construed as an amide-diimine in the formal Cr(III), S=3/2 formulation of **8**, the charge state of **9** is less well-defined. It is tempting to ascribe bia as a trianion in **9**, whose magnetic moment best describes an S=1 GS, but the carbon–nitrogen bonds adjacent to C19–C20 are 1.351(4) and 1.346(5) A, ⁴⁵ respectively, showing a significant amount of double bond character. The limiting Cr(IV) structure of (bia^{3–})-ClCr^{††}(CNAr')₂ may have significant mixing from (bia^{2-‡})-ClCr^{††}(CNAr')₂, i.e., a chromic center AF coupled to a bia radical dianion.

Calculations. *Rationale.* A crucial aspect of the chromium chemistry is the introduction of the pincer ligand, bida, which was chosen for this study partly because of its plausible redox noninnocence. This capability appeared to be manifested metrically via the aforementioned equation of charge (c = d(CN)ave -1.32 Å)/(-0.055)) and (c = d(CC) - 1.45 Å)/(0.025)). Consequently, calculations on representative molecules were conducted to assess the legitimacy of the metric rationale.

(bida)CrCl(PMe₂Ph) (1-PMe₂Ph). The geometry of (bida)-CrCl(PMe₂Ph) (1-PMe₂Ph) is reproduced quite well by hybrid DFT-MM calculations, with distances averaging within 0.012(15) Å of experiment, as shown in Figure 11a. With the parameters satisfactorily reproduced, Mulliken population analyses of these predominantly covalent compounds afforded an assessment of the spin densities. Figure 11b shows the core

of the quartet GS of (bida) CrCl(PMe₂Ph) (1-PMe₂Ph), which was assigned a configuration of (bida⁻¹) $^{\downarrow}$ Cr $^{\uparrow\uparrow\uparrow\uparrow}$ Cl(PMe₂Ph), i.e., high spin Cr(II) AF-coupled to the diamide radical anion, based on the experimental metrics and S=3/2 magnetic moment. With a spin density of +3.52 e⁻, the assignment of a Cr(II) GS is reasonable, but there is a modicum of opposing spin density (-0.44 e⁻) spread on the bida nitrogens and very little on the Cl and P. A conventional Cr(III) description, (bida⁻²)Cr $^{\uparrow\uparrow\uparrow}$ Cl(PMe₂Ph), is thus clearly within reason and also conforms to the $S_T=3/2$ criterion. The most apt description is an admixture of the two configurations, both of which lead to S=3/2 GS.

(bida)CrMe(THF) (2-Me). As an alternative to a halide derivative, (bida)CrMe(THF) (2-Me) was chosen as a formally Cr(III) derivative, and its calculated quartet GS geometry is illustrated in Figure 12a. Core bond distances are within 0.007(11) Å of their crystallographic equivalents, and the crucial angles are also quite close. The Mulliken spin densities numerically described in Figure 12b are similar to 1-PMe₂Ph, with Cr possessing a + 3.40 e⁻ value, and compensatory negative spin densities on the bida nitrogens (-0.217 e⁻ due to Cr) and the methyl (-0.23 e⁻). The conventional Cr(III) description, (bida⁻²)Cr^{↑↑↑}Me(THF), satisfies the calculational data and S = 3/2 GS. As the negative spin density is spread over several atoms, it is difficult to rationalize the bida radical anion Cr(II) alternative, (bida⁻¹) $^{\downarrow}$ Cr $^{\uparrow\uparrow\uparrow\uparrow}$ Cl(PMe₂Ph), suggested by the equation of

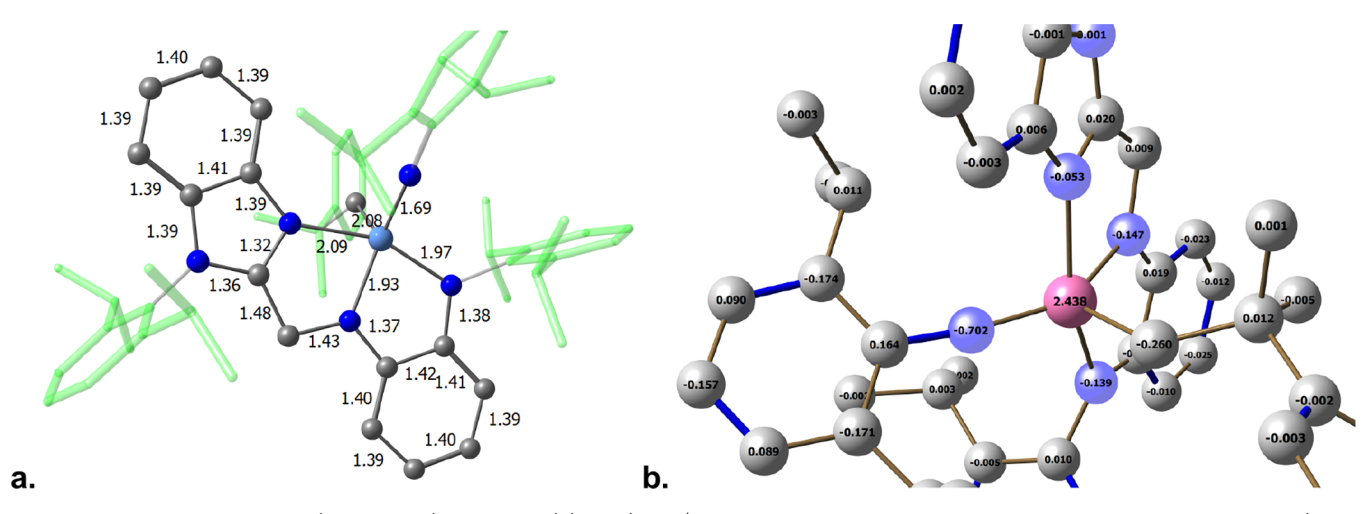


Figure 13. Calculated geometry (a, ONIOM(M06/6-31G(d):UFF), $2,6^{-i}$ Pr₂C₆H₃ groups in the MM partition, remainder in the QM region) and Mulliken spin densities (in e⁻) (b) of (bida)(PhMe₂CH₂)Cr=NAr (6=NAr) highlight atoms of consequence that indicate a plausible mix of Cr(III) and Cr(IV) states.

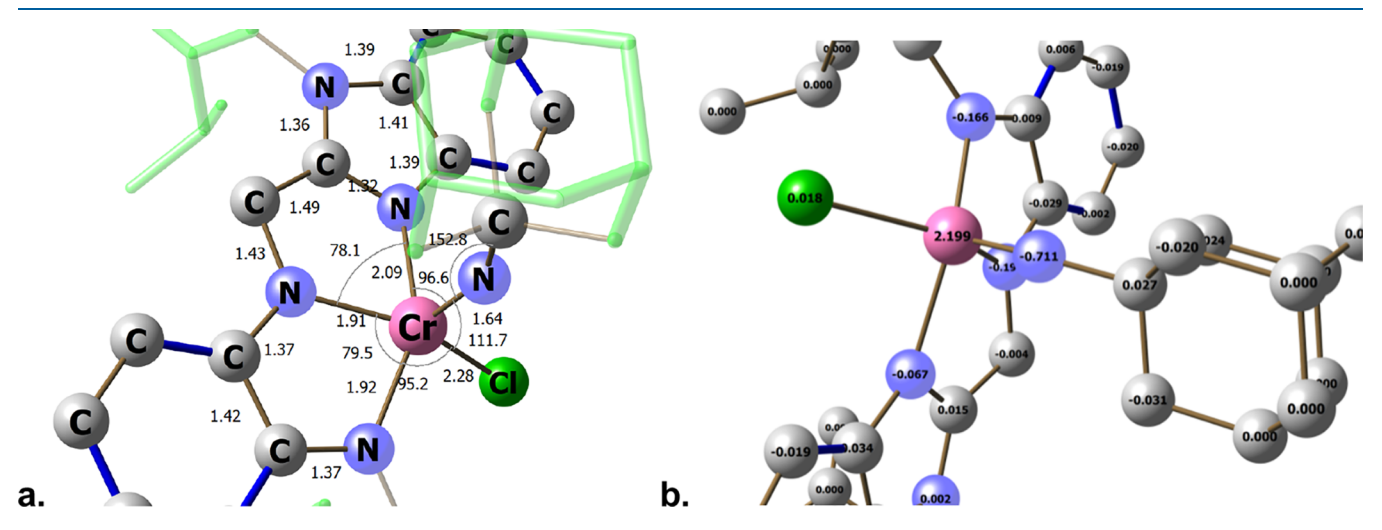


Figure 14. Calculated geometry (a, ONIOM(M06/6-31G(d):UFF), $2,6^{-i}$ Pr₂C₆H₃ groups in the MM partition, remainder in the QM region) and Mulliken spin densities (in e⁻) (b) of (bida)ClCr=NAd (3=NAd) highlighting atoms of consequence that are best construed as intermediate between integer representations of Cr(IV) or Cr(V) states.

charge. The spin density on the Me substituent draws a parallel to an effective ligand field B value, 48 as the greater field strength of the Me induces greater covalency and expansion of e^- -density about the Cr.

(bida)(PhMe₂CH₂)Cr=NAr (6=NAr). As shown in Figure 13a, the calculated geometry of the doublet GS of (bida)-(Nph)Cr=NAr (6=NAr) is portrayed, and the bond lengths deviate from the experiment by only 0.016(16) Å; hence, this appears to be a fairly accurate model of the S = 1/2 GS. Mulliken spin densities are illustrated in Figure 13b, and again, the calculations are somewhat indeterminate. The aforementioned experimental metric assessment suggested a configuration of (bida⁻¹)[↓](Nph)Cr^{↑↑}(=NAr), an anionic bida AFcoupled to an S = 1 Cr(IV) center for $S_T = 1/2$. Note that the metric assessment cannot evaluate imido or neophyl contributions, which are consequential in view of the calculations. Calculations reveal a Cr center with +2.44 e spin density, offset by $-0.34 e^-$ on the bida ligand nitrogens but more greatly offset by the imido nitrogen of -0.54 e (-0.702 + 0.164) and the neophyl α -carbon at -0.25 e (-0.26 + 0.01). At the face value, the nearest "integer"

assessment is $(bida^2-)(Nph)Cr^{\uparrow\uparrow}(NAr)^{\downarrow},$ but with the spin density so dispersed, minor contributions from $(bida^{-1})^{\downarrow}(Nph)Cr^{\uparrow\uparrow\uparrow}(NAr)^{\downarrow},$ where the spin density is smeared among the ligands, and a conventional Cr(V) $(bida)(Nph)Cr^{\uparrow}(NAr)$ are probable minor significant contributors.

(bida)ClCr=NAd (3=NAd). The structurally characterized adamantylimido-chloride (bida)ClCr=NAd (3=NAd) was chosen for calculational evaluation as a halide variant of the 6=NAr. Figure 14a reveals the core metrics of 3=NAd, whose calculated bond lengths average within 0.014(15) Å of the corresponding experimental values. Chromium has a Mulliken spin density (Figure 14b) of +2.20 e⁻, a value clearly more approximated by a d² Cr(IV) center, and the negative spin density is spread only modestly over the bida ligand (net $\sim -0.39 \text{ e}^-$), but mostly on the adamantyl imide (net -0.684). Somewhat surprisingly, the chloride has a tiny amount of positive spin density; hence, the most apt description is (bida²⁻)ClCr^{1†}(NAr)¹, conforming to an imidyl, and affording the GS $S_T = 1/2$ configuration. Note that while the imidyl character $^{36-38,71-74}$ of 3=NAd has not been directly

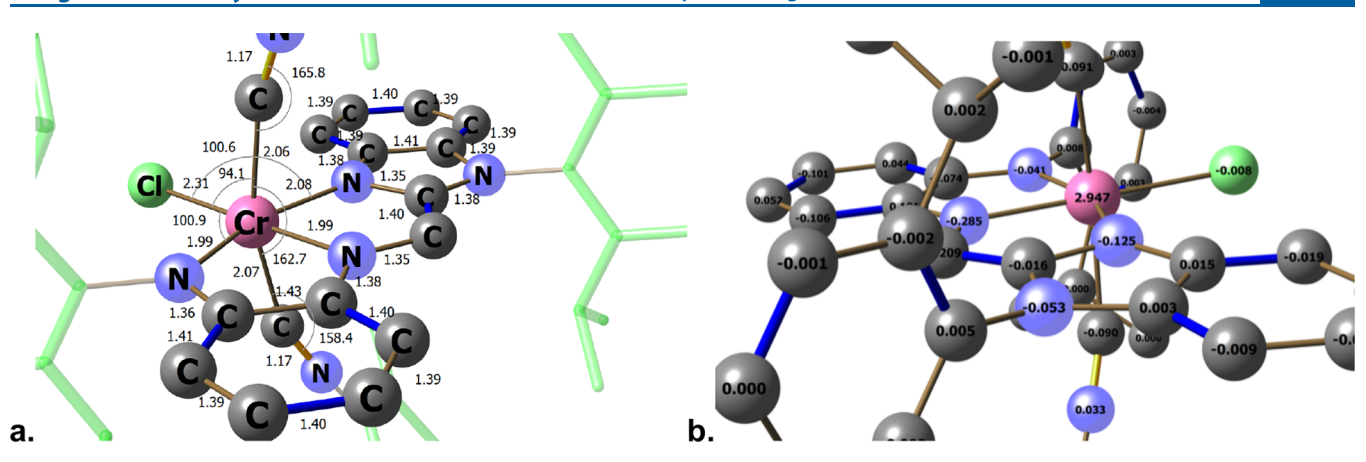


Figure 15. Calculated geometry (a, ONIOM(M06/6-31G(d):UFF), $2,6^{-i}$ Pr₂C₆H₃ groups in the MM partition, remainder in the QM region) and spin densities (in e⁻) (b) of (bia)ClCr(CNAr')₂ (9, Ar' = 2,6-Me₂C₆H₃) highlighting atoms of consequence that indicate are best construed as between Cr(III) and Cr(IV) states.

Scheme 6. Plausible Chain Process for (bida)CrCl(THF) (1-THF) to (bia)CrCl₂(THF) (8) Formation

Initiation:
$$\begin{array}{c} 2,6 \ ^{1}\text{Pr} \\ 2,6 \ ^{1}\text$$

observed, evidence of HAT to the imidyl nitrogen was obtained in its reaction with CNAr' ($Ar' = 2,6-Me_2C_6H_3$) to provide (bia) $CICr(CNAr')_2$ (9).

(bia)ClCr(CNAr')₂ (9). Recall that (bia)ClCr(CNAr')₂ (9, $Ar' = 2,6-Me_2C_6H_3$) possesses an ambiguity in the biaⁿ (n = -1, -2 (radical dianion), -3) ligand, which has at least three plausible redox states. Examination of the calculated distances within the core shown in Figure 15a reveals that they average within 0.009(9) Å of the values determined from X-ray crystallography, and the angles show similar accuracy. The chromium Mulliken spin density illustrated in Figure 15b is +2.95 e⁻, a value that can be interpreted as $(bia^{2-})^{\downarrow}ClCr^{\uparrow\uparrow\uparrow}(CNAr')_{2}\text{, but there is a substantial amount}$ of negative spin density on bia ($\sim -0.62 \text{ e}^-$), and small amounts on the isocyanides (-0.012 e^-) and Cl (-0.068 e^-) . Considerable triamide Cr(IV) character, i.e., (bia³⁻)- $ClCr^{\uparrow\uparrow}(CNAr')_{2}$ must be considered in view of this spin density dispersion. The summation of experimental and computational data implicates 9 as being between Cr(III) and Cr(IV) integer species.

CONCLUSIONS

Serendipitous discovery of the previously unknown pincer ligand bida enabled its study as applied to chromium in varied formal oxidation states. Three types of ligand activity were anticipated: (1) redox noninnocence (RNI) of the diamide backbone (i.e., (bida)ⁿ, n = 0, 1, 2), (2) H atom or proton loss from the backbone methylene, and (3) hemilability of the benzimidazole N-donor group.

Metric parameters intrinsic to the phenylene-diamide section of bida appear remarkably consistent even when the chromic centers of (bida)(R/X)CrL are oxidized to the formal Cr(V) variants (bida)(R/X)Cr = NR'. The phenomenological equations of charge (i.e., c = d(CN)ave -1.32 Å)/(-0.055)) and (c = d(CC) - 1.45 Å)/(0.025)) developed from (bida)Na₂(THF) metrics in conjunction with common Ar–N distances, etc. afford average charges of -1.08(2) and -1.06(22). Noticeably, the experimental charge arguments reveal bida to have roughly the same charge whether attached to formally Cr(III) or Cr(V),

Calculationally the bida ligand shows ambiguity, which the dianion form manifests to a greater extent than the monoanion. The conventionally described Cr(III) species, (bida)CrCl-(PMe₂Ph) (1-PMe₂Ph) and (bida)CrMe(THF) (2-Me), have spin densities $\sim +3.5$ e⁻, roughly between a d³ and d⁴ configurations, and the remainder of the spin density is delocalized over all the neighboring atoms. Conventional Cr(V) imides have spin densities $\sim +2.3$ e⁻, close to a d² configuration, with contributions from d³ states not wholly unreasonable. Surprisingly, bida does little electronic buffering via its π -system, taking a backseat to the imido ligand that is best construed as an imidyl, $^{36-38,71-74}$ with about -0.7 e⁻ of spin density. With the inferred HAT chemistry in the production of (bia)ClCr(CNAr')₂ (9, Ar' = 2,6-Me₂C₆H₃) from (bida)ClCr=NAd (3=NAd) in the presence of 2,6-Me₂C₆H₃NC, its imidyl character is apparently consequential enough to afford some reactivity.

Thermal studies of (bida)R'Cr=NR (R' = Me, R = Ad, Ar, 5=NR; R' = CH₂CMe₂Ph (Nph), R = Ad, Ar, 6 = NR) failed to elicit the relatively uncommon migratory insertion of an alkyl into an imide. Given the predicted imidyl character, this functionality may not be electrophilic enough and/or the alkyl is not nucleophilic enough to permit migration. With the R'/NR angles at $\geq 100^{\circ}$, and significant sterics about the Cr, the requisite geometry to access insertion might also be difficult. Insertion of the ArN₃ (Ar = 2,6-iPr₂-C₆H₃) terminal nitrogen did occur, but the incipient (bida)(Nph)Cr=N-N=NAr intermediate is likely to be far more electrophilic at nitrogen and have lesser steric issues due to the distal Ar group on the azide, ultimately shown in the κ^2 -binding arrangement observed in (bida)Cr(κ^2 -N,N-ArN₃neophyl) (7).

The oxidation study with NCS shown in Scheme 5 can be plausibly rationalized as the chlorination of (bida)CrCl(THF) (1-THF), via the chain process in Scheme 6. Chlorination of 1-THF can generate conventional Cr(IV) (bida)CrCl₂(THF) and the succinimide radical. While these can combine within a solvent cage to afford (bia)CrCl₂(THF) (8) and succinimide, radical escape from the cage allows it to undergo HAT with 1-THF to produce the formal Cr(II) as (bia)CrCl(THF). As a Cr(II) intermediate, it is more likely to abstract Cl atom from NCS to afford product 8 and regenerate the propagating radical in a standard chain process.

In conclusion, if the bida ligand is manifesting RNI, its metric parameters are not reflecting the changes in charge; hence, its electronic buffering capacity may be occurring via its sigma-donation, i.e., its covalency in σ -bonding (see plotted molecular orbitals in the Supporting Information). It is apparent that the spin densities and charge assessments belie the conventional approach of interpreting charge distribution in integer terms. Moreover, observations of unconventional $\mu_{\rm eff}$ values and featureless EPR spectra appear to coincide with the smearing of electron density in AF-coupled systems and should be recognized as potential signatures of RNI when metric parameters are inconclusive or unobtainable.

ASSOCIATED CONTENT

Supporting Information

The Supporting Information is available free of charge at https://pubs.acs.org/doi/10.1021/acs.inorgchem.3c01771.

Experimental details on all procedures, spectroscopic data, calculational information, and X-ray crystallographic information pertaining to (bida)Na₂ (CCDC-

2266143), 1-PMe₂Ph (CCDC-2266144), 2-Me (CCDC-2266145), 2-Nph (CCDC-2266146), 3=NAd (CCDC-2266147), 4=NAr (CCDC-2266148), 5=NAr (CCDC-2266149), 6=NAr (CCDC-2266150), 7 (CCDC-2266151), 8 (CCDC-2266152), and 9 (CCDC-2266153) (PDF)

Accession Codes

CCDC 2266143–2266153 contain the supplementary crystallographic data for this paper. These data can be obtained free of charge via www.ccdc.cam.ac.uk/data_request/cif, or by emailing data_request@ccdc.cam.ac.uk, or by contacting The Cambridge Crystallographic Data Centre, 12 Union Road, Cambridge CB2 1EZ, UK; fax: +44 1223 336033.

AUTHOR INFORMATION

Corresponding Author

Peter T. Wolczanski — Department of Chemistry and Chemical Biology, Baker Laboratory Cornell University, Ithaca, New York 14853, United States; orcid.org/0000-0003-4801-0614; Email: ptw2@cornell.edu

Authors

Ann K. Kayser – Department of Chemistry and Chemical Biology, Baker Laboratory Cornell University, Ithaca, New York 14853, United States; orcid.org/0000-0002-7933-4163

Thomas R. Cundari — Department of Chemistry, CASCam University of North Texas Denton, Denton, Texas 76201, United States; orcid.org/0000-0003-1822-6473

Samantha N. MacMillan – Department of Chemistry and Chemical Biology, Baker Laboratory Cornell University, Ithaca, New York 14853, United States; occid.org/0000-0001-6516-1823

Melissa M. Bollmeyer — Department of Chemistry and Chemical Biology, Baker Laboratory Cornell University, Ithaca, New York 14853, United States; Department of Chemistry, CASCam University of North Texas Denton, Denton, Texas 76201, United States

Complete contact information is available at: https://pubs.acs.org/10.1021/acs.inorgchem.3c01771

Notes

The authors declare no competing financial interest.

ACKNOWLEDGMENTS

PTW and TRC acknowledge the National Science Foundation for funding this work (CHE-1953884, CHE-1953547, CHE-1531468), and the support of Cornell University. We thank Lisa Gong for help in isolating and characterizing 4 = NAr, and Prof. Kyle M. Lancaster for help in fitting EPR spectra. EPR studies reported in this publication were supported by the National Institute of General Medical Sciences of the National Institutes of Health under Award Number 1R24GM146107.

■ REFERENCES

- (1) Hulley, E. B.; Wolczanski, P. T.; Lobkovsky, E. B. Carbon-carbon Bond Formation from Azaallyl and Imine Couplings About Metalmetal Bonds. *J. Am. Chem. Soc.* **2011**, *133*, 18058–18061.
- (2) Frazier, B. A.; Williams, V. A.; Wolczanski, P. T.; Bart, S.; Meyer, K.; Cundari, T. R.; Lobkovsky, E. B. C-C Bond Formation and Related Reactions at the CNC Backbone in (smif)FeX (smif = 1,3-di-(2-pyridyl)-2-azaallyl): Dimerizations, 3 + 2 Cyclization, and Nucleophilic Attack; Transfer Hydrogenations and Alkyne Trimeriza-

- tion $(X = N(TMS)_2, dpma (di-(2-pyridyl-methyl)-amide))$. *Inorg. Chem.* **2013**, 52, 3295–3312.
- (3) Frazier, B. A.; Wolczanski, P. T.; Keresztes, I.; DeBeer, S.; Lobkovsky, E. B.; Pierpont, A. W.; Cundari, T. R. Synthetic Approaches to (smif)₂Ti (smif = 1,3-di-(2-pyridyl)-2-azaallyl) Reveal Redox Non-Innocence and C-C Bond-Formation. *Inorg. Chem.* **2012**, *51*, 8177–8186.
- (4) Morris, W. D.; Wolczanski, P. T.; Sutter, J.; Meyer, K.; Cundari, T. R.; Lobkovsky, E. B. Iron and Chromium Complexes Containing Tridentate Chelates Based on Nacnac and Imino- and Methyl-Pyridine Components: Triggering C-C(X) Bond Formation. *Inorg. Chem.* **2014**, *53*, 7467–7484.
- (5) Volpe, E. C.; Wolczanski, P. T.; Darmon, J. M.; Lobkovsky, E. B. Syntheses and Characterizations of α -Iminopyridine Compounds (AlkylN = CHpy)₂Fe(L/ X_n), and an Assessment of Redox Non-Innocence. *Polyhedron* **2013**, *52*, 406–415.
- (6) Hulley, E. B.; Williams, V. A.; Morris, W. D.; Wolczanski, P. T.; Hernández-Burgos, K.; Lobkovsky, E. B.; Cundari, T. R. Disparate Reactivity from Isomeric {Me₂C(CH₂N = CHpy)₂} and {Me₂C(CH = NCH₂py)₂} Chelates in Iron Complexation. *Polyhedron* **2014**, *84*, 182–191.
- (7) Williams, V. A.; Hulley, E. B.; Wolczanski, P. T.; Lancaster, K. M.; Lobkovsky, E. B. Pushing the limits of redox non-innocence: pseudo square planar $[\{\kappa^4\text{-Me}_2C(CH_2N=CHpy)_2\}Ni]^n$ (n = 2+, 1+, 0, -1, -2) favor Ni(II). *Chem. Sci.* **2013**, *4*, 3636–3648.
- (8) Lindley, B. M.; Wolczanski, P. T.; Cundari, T. R.; Lobkovsky, E. B. 1st Row Transition Metal and Lithium Pyridine-ene-amide Complexes Exhibiting N- and C-Isomers and Ligand-based Activation of Benzylic C-H Bonds. *Organometallics* **2015**, *34*, 4656–4688.
- (9) Hulley, E. B.; Heins, S. P.; Wolczanski, P. T.; Lancaster, K. M.; Lobkovsky, E. B. Azaallyl-derived ring formation via redox coupling in first row transition metals. *Polyhedron* **2019**, *158*, 225–233.
- (10) Jacobs, B. P.; Wolczanski, P. T.; Lobkovsky, E. B. Oxidatively Triggered Carbon-Carbon Bond Formation in Ene-amide Complexes. *Inorg. Chem.* **2016**, *55*, 4223–4232.
- (11) Heins, S. P.; Zhang, B.; MacMillan, S. N.; Cundari, T. R.; Wolczanski, P. T. Oxidative Additions to Ti(IV) in [(dadi)⁴]-Ti^{IV}(THF) Involve Carbon-Carbon Bond Formation and Redox-Noninnocent Behavior. *Organometallics* **2019**, *38*, 1502–1515.
- (12) Heins, S. P.; Morris, W. D.; Cundari, T. R.; MacMillan, S. N.; Lobkovsky, E. B.; Livezey, N.; Wolczanski, P. T. Complexes of [(dadi)Ti(L/X)]^m that Reveal Redox Non-innocence, and a Stepwise Carbene Insertion into a Carbon-carbon Bond. *Organometallics* **2018**, 37, 3488–3501. (c)
- (13) Luca, O. R.; Crabtree, R. H. Redox Ligands in Catalysis. *Coord. Chem. Rev.* **2013**, 42, 1440–1459.
- (14) Caulton, K. G. Systematics and Future Projections Concerning Redox-Noninnocent Amide/Imine Ligands. *Eur. J. Inorg. Chem.* **2012**, 2012, 435–443.
- (15) Budzelaar, P. H. M. Radical Chemistry of Iminepyridine Ligands. Eur. J. Inorg. Chem. 2012, 2012, 530-534.
- (16) Berben, L. A.; de Bruin, B.; Heyduk, A. G. Non-innocent ligands. *Chem. Commun.* **2015**, *51*, 1553–1554.
- (17) (a) Lyaskovskyy, V.; de Bruin, B. Redox Non-Innocent Ligands: Versatile New Tools to Control Catalytic Reactions. *ACS Catal.* **2012**, *2*, 270–279. (b) Dzik, W. I.; van der Vlugt, J. I.; Reek, J. N. H.; de Bruin, B. Ligands that Store and Release Electrons During Catalysis. *Angew. Chem., Int. Ed.* **2011**, *50*, 3356–3358.
- (18) Munhá, R. F.; Zarkesh, R. A.; Heyduk, A. F. Group transfer reactions of d⁰ transition metal complexes: redox-active ligands provide a mechanism for expanded reactivity. *Dalton Trans.* **2013**, *42*, 3751–3766.
- (19) van Leest, N. P.; Epping, R. F. J.; van Vliet, K. M.; Lankelma, M.; van den Heuvel, E. J.; Heijbrink, N.; Broersen, R.; de Bruin, B. Single-Electron Elementary Steps in Homogeneous Organometallic Catalysis. *Adv. Organomet. Chem.* **2018**, *70*, 71–180.
- (20) Lu, C. C.; Bill, E.; Weyhermüller, T.; Bothe, E.; Wieghardt, K. Neutral Bis(α-iminopyridine)metal Complexes of the First-Row Transition Ions (Cr, Mn, Fe, Co, Ni, Zn) and Their Monocationic

- Analogues: Mixed Valency Involving a Redox Noninnocent Ligand System. J. Am. Chem. Soc. 2008, 130, 3181–3197.
- (21) Pokhriyal, D.; Heins, S. P.; Sifri, R. J.; Genetekos, D. T.; Coleman, R. E.; Wolczanski, P. T.; Fors, B. P.; Cundari, T. R.; Lancaster, K. M.; MacMillan, S. N. Reversible C-C Bond Formation, Halide Abstraction, and Electromers in Complexes of Iron Containing Redox Noninnocent Pyridine-imine Ligands. *Inorg. Chem.* **2021**, *60*, 18662–18673.
- (22) Heins, S. P.; Morris, W. D.; Wolczanski, P. T.; Lobkovsky, E. B.; Cundari, T. R. Nitrene Insertion into CC and CH Bonds of Diamide-diimine Ligated Chromium and Iron Complexes. *Angew. Chem., Int. Ed.* **2015**, *54*, 14407–14411.
- (23) Heins, S. P.; Wolczanski, P. T.; Cundari, T. R.; MacMillan, S. N. Redox non-innocence permits catalytic nitrene carbonylation by (dadi)Ti = NAd (Ad = adamantyl). *Chem. Sci.* **2017**, *8*, 3410–3418. (24) (a) Beaumier, E. P.; Billow, B. S.; Singh, A. K.; Biros, S. M.;
- Odom, A. L. A Complex with Nitrogen Single, Double, and Triple Bonds to the Same Chromium Atom: Synthesis, Structure, and Reactivity. *Chem. Sci.* **2016**, *7*, 2532–2536. (b) Ciszewski, J. T.; Harrison, J. F.; Odom, A. L. Investigation of Transition Metal–Imido Bonding in M(NBu^t)₂(dpma). *Inorg. Chem.* **2004**, *43*, 3605–3617.
- (25) Liu, S.; Jung, J.; Ohkubo, K.; Hicks, S. D.; Bougher, C. J.; Abu-Omar, M. M.; Fukuzumi, S. Activationless Electron Self-Exchange of High-Valent Oxo and Imido Complexes of Chromium Corroles. *Inorg. Chem.* **2015**, *54*, 9223–9228.
- (26) Lu, C. C.; Debeer, S. G.; Weyhermuller, T.; Bill, E.; Bothe, E.; Wieghardt, K. An Electron-Transfer Series of High-Valent Chromium Complexes with Redox Non-Innocent, Non-Heme Ligands. *Angew. Chem., Int. Ed.* **2008**, 47, 6384–6387.
- (27) Yousif, M.; Tjapkes, D. J.; Lord, R. L.; Groysman, S. Catalytic Formation of Asymmetric Carbodiimides at Mononuclear Chromium(II/IV) Bis(Alkoxide) Complexes. *Organometallics.* **2015**, 34, 5119–5128.
- (28) Panyam, P. K. R.; Stöhr, L.; Wang, D.; Frey, W.; Buchmeiser, M. R. Chromium(VI) Bisimido Dichloro, Bisimido Alkylidene, and Chromium(V) Bisimido Iodo N-Heterocyclic Carbene Complexes. *Eur. J. Inorg. Chem.* **2020**, 2020, 3673–3681.
- (29) Jandciu, E. W.; Legzdins, P.; McNeil, W. S.; Patrick, B. O.; Smith, K. M. Cr(NAr)(O)(NPrⁱ₂)(Ar): A Strongly-Bent Monoimido Complex Resulting from Nitrosyl Ligand Cleavage. *Chem. Commun.* **2000**, *18*, 1809–1810.
- (30) Tsai, Y. C.; Wang, P. Y.; Chen, S. A.; Chen, J. M. Inverted-Sandwich Dichromium(I) Complexes Supported by Two β -Diketiminates: A Multielectron Reductant and Syntheses of Chromium Dioxo and Imido. *J. Am. Chem. Soc.* **2007**, *129*, 8066—8067.
- (31) Wu, P.; Yap, G. P. A.; Theopold, K. H. Structure and Reactivity of Chromium(VI) Alkylidenes. *J. Am. Chem. Soc.* **2018**, 140, 7088–7091
- (32) Rufanov, K. A.; Kipke, J.; Sundermeyer, J. Sulfinylamine Metathesis at Oxo Metal Species Convenient Entry into Imido Metal Chemistry. *Dalton Trans.* **2011**, *40*, 1990–1997.
- (33) Leung, W. H. Synthesis and Reactivity of Organoimido Complexes of Chromium. Eur. J. Inorg. Chem. 2003, 2003, 583-593.
- (34) Siemeling, U.; Kölling, L.; Kuhnert, O.; Neumann, B.; Stammler, A.; Stammler, H. G.; Fink, G.; Kaminski, E.; Kiefer, A.; Schrock, R. R. Transition Metal Complexes Containing Functionalized Organoimido and Phosphaneiminato Ligands. *Z. Anorg. Allg. Chem.* 2003, 629, 781–792.
- (35) Sydora, O. L.; Kuiper, D. S.; Wolczanski, P. T.; Lobkovsky, E. B.; Dinescu, A.; Cundari, T. R. The Butterfly Dimer [(tBu_3SiO)-Cr]₂(μ -OSi tBu_3)₂ and Its Oxidative Cleavage to (tBu_3SiO)₂Cr(=N-N = CPh₂)₂ and (tBu_3SiO)₂Cr = N(2,6-Ph₂-C₆H₃). *Inorg. Chem.* **2006**, 45, 2008–2021.
- (36) Wilding, M. J. T.; Iovan, D. A.; Wrobel, A. T.; Lukens, J. T.; Macmillan, S. N.; Lancaster, K. M.; Betley, T. A. Direct Comparison of C-H Bond Amination Efficacy through Manipulation of Nitrogen-Valence Centered Redox: Imido versus Iminyl. *J. Am. Chem. Soc.* **2017**, 139, 14757–14766.

- (37) Dong, Y.; Clarke, R. M.; Zheng, S. L.; Betley, T. A. Synthesis and Electronic Structure Studies of a Cr-Imido Redox Series. *Chem. Commun.* **2020**, *56*, 3163–3166.
- (38) Zhou, W.; Patrick, B. O.; Smith, K. M. Influence of Redox Non-Innocent Phenylenediamido Ligands on Chromium Imido Hydrogen-Atom Abstraction Reactivity. *Chem. Commun.* **2014**, *50*, 9958–9960.
- (39) Coles, M. P.; Gibson, V. C.; Clegg, W.; Elsegood, M. R. J.; Porrelli, P. A. Synthesis and Reactivity of the First Stable Chromium(VI) Alkylidene Complexes. *Chem. Commun.* **1996**, *16*, 1963–1964.
- (40) (a) Wu, P.; Yap, G. P. A.; Theopold, K. H. Synthesis, Characterization, and Reactivity of Chromium(VI) Alkylidenes. *Organometallics* **2019**, 38, 4593–4600. (b) Wu, P.; Yap, G. P. A.; Theopold, K. H. Structure and Reactivity of Chromium(VI) Alkylidenes. *J. Am. Chem. Soc.* **2018**, 140, 7088–7091.
- (41) Herebian, D.; Wieghardt, K. E.; Neese, F. Analysis and Interpretation of Metal-Radical Coupling in a Series of Square Planar Nickel Complexes: Correlated Ab Initio and Density Functional Investigation of $[Ni(L^{ISQ})_2]$ ($L^{ISQ}=3,5$ -Di-Tert-Butyl-o-Diiminobenzosemiquinonate(1-)). J. Am. Chem. Soc. 2003, 125, 10997–11005.
- (42) Bill, E.; Bothe, E.; Chaudhuri, P.; Chlopek, K.; Herebian, D.; Kokatam, S.; Ray, K.; Weyhermüller, T.; Neese, F.; Wieghardt, K. Molecular and Electronic Structure of Four- and Five-Coordinate Cobalt Complexes Containing Two o-Phenylenediamine- or Two o-Aminophenol-Type Ligands at Various Oxidation Levels: An Experimental, Density Functional, and Correlated ab initio Study. Chem. Eur. J. 2005, 11, 204–224.
- (43) Herebian, D.; Bothe, E.; Neese, F.; Weyhermüller, T.; Wieghardt, K. Molecular and Electronic Structures of Bis-(o-Diiminobenzosemiquinonato)Metal(II) Complexes (Ni, Pd, Pt), Their Monocations and -Anions, and of Dimeric Dications Containing Weak Metal-Metal Bonds. J. Am. Chem. Soc. 2003, 125, 9116–9128
- (44) Chłopek, K.; Bothe, E.; Neese, F.; Weyhermuller, T.; Wieghardt, K. Molecular and Electronic Structures of Tetrahedral Complexes of Nickel and Cobalt Containing N,N',-Disubstituted, Bulky o- Diiminobenzosemiquinonate(1-) π -Radical Ligands. *Inorg. Chem.* **2006**, *45*, 6298–6307.
- (45) Allen, F. H.; Kennard, O.; Watson, D. G.; Orpen, A. G.; Brammer, L.; Taylor, R. Tables of Bond Lengths determined by X-Ray and Neutron Diffraction. Part 1. Bond Lengths in Organic Compounds. J. Chem. Soc., Perkin Trans. II 1987, S1–S19.
- (46) Kern, R. J. Tetrahydrofuran Complexes of Transition Metal Chlorides. J. Inorg. Nucl. Chem. 1962, 24, 1105–1109.
- (47) (a) Evans, D. F. The Determination of the Paramagnetic Susceptibility of Substances in Solution by Nuclear Magnetic Resonance. J. Chem. Soc. 1959, 2003–2005. (b) Schubert, E. M. Utilizing the Evans Method with a Superconducting NMR Spectrometer in the Undergraduate Laboratory. J. Chem. Educ. 1992, 69, 62.
- (48) Figgis, B. N.; Hitchman, M. A. Ligand Field Theory and Its Applications; Wiley-VCH: New York, 2000.
- (49) Addison, A. W.; Rao, N. T.; Reedijk, J.; van Rijn, J.; Verschoor, G. C. Synthesis, structure, and spectroscopic properties of copper(II) compounds containing nitrogen—sulphur donor ligands; the crystal and molecular structure of aqua[1,7-bis(N-methylbenzimidazol-2'-yl)-2,6-dithiaheptane] copper(II) perchlorate. J. Chem. Soc., Dalton Trans. 1984, 1349—1356.
- (50) Matsumoto, T.; Yamamoto, R.; Wakizaka, M.; Nakada, A.; Chang, H.-C. Molecular Insights into the Ligand-Based Six-Proton-and Six-Electron-Transfer Processes Between Tris-ortho-Phenylenediamines and Tris-ortho-Benzoquinodiimines. Chem. Eur. J. 2020, 26, 9609—9619.
- (51) Brown, S. N. Metrical Oxidation States of 2-Amidophenoxide and Catecholate Ligands: Structural Signatures of Metal-Ligand π -Bonding in Potentially Noninnocent Ligands. *Inorg. Chem.* **2012**, *51*, 1251–1260.

- (52) (a) Marshall-Roth, T.; Brown, S. N. Redox activity and π bonding in a tripodal seven-coordinate mollybdenum(VI) tris-(amidophenolate). *Dalton Trans.* **2015**, 44, 677–685. (b) Ranis, L. G.; Werellapatha, K.; Pietrini, N. J.; Bunker, B. A.; Brown, S. N. Metal and Ligand Effects on Bonding in Group 6 Complexes of Redox-Active Amidophenoxides. *Inorg. Chem.* **2014**, 53, 10203–10206. (c) Randolph, A. H.; Seewald, N. J.; Karl, R.; Brown, S. N. Tris(3,5-di-tert-butylcatecholato)molybdenum(VI): Lewis Acidity and Nonclasical Oxygen Atom Transfer. *Inorg. Chem.* **2013**, 52, 12587–12598. (53) Marshall-Roth, T.; Yao, K.; Parkhill, J. A.; Brown, S. N. On the border between localization and delocalization: tris(iminooxolene)-titanium(iv). *Dalton Trans.* **2019**, 48, 1427–1435.
- (54) Conner, K. M.; Perugini, A. L.; Malabute, M.; Brown, S. N. Group 10 Bis(iminosemiquinone) Complexes: Measurement of Singlet-Triplet Gaps and Analysis of the Effects of Metal and Geometry on Electronic Structure. *Inorg. Chem.* **2018**, *57*, 3272–3286
- (55) Hoffman, J. M.; Oliver, A. G.; Brown, S. N. The Metal or the Ligand? The Preferred Locus for Redox Changes in Oxygen Atom Transfer Reactions of Rhenium Amidodiphenoxides. *J. Am. Chem. Soc.* **2017**, *139*, 4521–4531.
- (56) Orpen, A. G.; Brammer, L.; Allen, F. H.; Kennard, O.; Watson, D. G.; Taylor, R. Tables of Bond Lengths determined by X-Ray and Neutron Diffraction. Part 2. Organometallic Compounds and Coordination Complexes of the d- and f-Block Metals. *J. Chem. Soc., Dalton Trans.* 1989, S1–S83.
- (57) (a) Qi Liu, Q.; Tor, Y. Simple Conversion of Aromatic Amines into Azides. *Org. Lett.* **2003**, *5*, 2571–2572. (b) Treitler, D. S.; Leung, S. How Dangerous Is Too Dangerous? A Perspective on Azide Chemistry. *J. Org. Chem.* **2022**, *87*, 11293–11295.
- (58) Devore, D. D.; Lichtenhan, J. D.; Takusagawa, F.; Maata, E. A. Complexes of (Arylimido)vanadium(V). Synthetic, Structural, Spectroscopic, and Theoretical Studies of V(Ntol)Cl₃ and Derivatives. *J. Am. Chem. Soc.* **1987**, *109*, 7408–74416.
- (59) (a) Kawamoto, Y.; Elser, I.; Buchmeiser, M. R.; Nomura, K. Vanadium(V) Arylimido Alkylidene N-Heterocyclic Carbene Alkyl and Perhalophenoxy Alkylidenes for the Cis, Syndiospecific Ring Opening Metathesis Polymerization of Norbornene. Organometallics 2021, 40, 2017-2022. (b) Hatagami, K.; Nomura, K. Synthesis of (Adamantylmido)vanadium(V)-Alkyl, Alkylidene Complex Trapped with PMe3: Reactions of the Alkylidene Complexes with Phenols. Organometallics 2014, 33, 6585-6592. (c) Chaimongkolkunasin, S.; Nomura, K. (Arylimido) Vanadium (V)-Alkylidenes Containing Chlorinated Phenoxy Ligands: Thermally Robust, Highly Active Catalyst in Ring-Opening Metathesis Polymerization of Cyclic Olefins. Organometallics 2018, 37, 2064-2074. (d) Hou, X. H.; Nomura, K. (Arylimido)vanadium(V)-Alkylidene Complexes Containing Fluorinated Aryloxo and Alkoxo Ligands for Fast Living Ring-Opening Metathesis Polymerization (ROMP) and Highly Cis-Specific ROMP. J. Am. Chem. Soc. 2015, 137, 4662-4665. (e) Chaimongkolkunasin, S.; Nomura, K. (Arylimido)Vanadium(V)-Alkylidenes Containing Chlorinated Phenoxy Ligands: Thermally Robust, Highly Active Catalyst in Ring-Opening Metathesis Polymerization of Cyclic Olefins. Organometallics 2018, 37, 2064-2074.
- (60) Jacobs, B. P.; Wolczanski, P. T.; Jiang, Q.; Cundari, T. R.; MacMillan, S. N. Rare Examples of Fe(IV) Alkyl-Imide Migratory Insertions: Impact of Fe-C Covalency in $(Me_2IPr)Fe(=NAd)R_2$ (R = ^{neo}Pe , 1-nor). *J. Am. Chem. Soc.* **2017**, *139*, 12145–12148.
- (61) Cundari, T. R.; Jacobs, B. P.; MacMillan, S. N. Dispersion Forces Play a Role in $(Me_2IPr)Fe(=NAd)R_2$ (Ad = adamantyl; R = ^{neo}Pe , 1-nor) Insertions and BDEs. *Dalton Trans.* **2018**, 47, 6025–6030.
- (62) Hu, X.; Meyer, K. Terminal Cobalt(III) Imido Complexes Supported by Tris(Carbene) Ligands: Imido Insertion into the Cobalt—Carbene Bond. *J. Am. Chem. Soc.* **2004**, *126*, 16322–16323. (63) (a) Matsunaga, P. T.; Hess, C. R.; Hillhouse, G. L. Reactions of
- (63) (a) Matsunaga, P. T.; Hess, C. R.; Hillhouse, G. L. Reactions of Organoazides with Nickel Alkyls. Syntheses and Reactions of Nickel(II) Amido Complexes. *J. Am. Chem. Soc.* **1994**, *116*, 3665—3666. (b) Koo, K.; Hillhouse, G. L. Indoline Synthesis via Coupling of

- Phenethyl Grignard Reagents with Organoazides Mediated by (Alkylphosphine)nickel(II) Complexes. *Organometallics* **1996**, *15*, 2669–2271.
- (64) Cenini, S.; Gallo, E.; Caselli, A.; Ragaini, F.; Fantauzzi, S.; Piangiolino, C. Coordination chemistry of organic azides and amination reactions catalyzed by transition metal complexes. *Coord. Chem. Rev.* **2006**, 250, 1234–1253.
- (65) Reinholdt, A.; Kwon, S.; Jafari, M. G.; Gau, M. R.; Caroll, P. J.; Lawrence, C.; Gu, J.; Baik, M. H.; Mindiola, D. J. An Isolable Azide Adduct of Titanium(II) Follows Bifurcated Deazotation Pathways to an Imide. J. Am. Chem. Soc. 2022, 144, 527–537.
- (66) Lin, K. M.; Wang, P. Y.; Shieh, Y. J.; Chen, H. Z.; Kuo, T. S.; Tsai, Y. C. Reductive N-N Bond Cleavage and Coupling of Organic Azides Mediated by Chromium(i) and Vanadium(i) β -Diketiminate. New J. Chem. **2010**, 34, 1737–1745.
- (67) Moore, D. S.; Robinson, S. D. Catenated Nitrogen Ligands Part I. Transition Metal Derivatives of Triazenes, Tetrazenes, Tetrazadienes, and Pentazadienes. *Adv. Inorg. Chem. Radiochem.* **1986**, 30, 1–68.
- (68) Chisholm, M. H.; Haitko, D. A.; Huffman, J. C.; Folting, K. The Molybdenum-Molybdenum Triple Bond. 7. Bis (1,3-di-*p*-tolyltrazenido)tetrakis (dimethylamido)dimolybdenum. *Inorg. Chem.* **1981**, 20, 171–174.
- (69) Brown, L. D.; Ibers, J. A. Structural Studies of Triazenido Complexes. 1. Crystal and Molecular Structure of *trans*-Bis-(triphenylphosphine) carbonyl(1,3-di-p-tolyltriazenido)-hydridoruthenium(II), *trans*-[Ru(H)(CH₃C₆H₄N₃C₆H₄CH₃)(CO)-(P(C₆H₅)₃)₂. *Inorg. Chem.* **1976**, 15, 2788–2793.
- (70) (a) Schwitalla, K.; Lee, W.; Fischer, M.; Schmidtmann, M.; Beckhaus, R. Synthesis and Characterization of Zr and Hf Triazenido Complexes with Rare κ1-N-Coordination Built Directly in the Coordination Sphere of the Metal. *Organometallics* **2023**, 42, 1259–1266. (b) Zarkesh, R. A.; Heyduk, A. F. Reactivity of Organometallic Tantalum Complexes Containing a Bis(phenoxy)amide (ONO)³-Ligand with Aryl Azides and 1,2-diphenylhydrazine. *Organometallics* **2011**, 30, 4890–4898. (c) Li, B.; Huse, K.; Wölper, C.; Schulz, S. Synthesis and reactivity of heteroleptic zinc(I) complexes toward heteroallenes. *Chem. Commun.* **2021**, 57, 13692–13695. (d) Mills, D. P.; Soutar, L.; Cooper, O. J.; Lewis, W.; Blake, A. J.; Liddle, S. T. Reactivity of the Yttrium Akyl Carbene Complex [Y(BIPM)-(CH₂C₆H₅)(THF)] (BIPM = {C(PPh₂NSiMe₃)₂})²: From Insertions, Substitutions, and Additions to Nontypical Transformations. *Organometallics* **2013**, 32, 1251–1264.
- (71) Zdilla, M. J.; Abu-Omar, M. M. Mechanism of Catalytic Aziridination with Manganese Corrole: The Often Postulated High-Valent Mn(V) Imido Is Not the Group Transfer Reagent. *J. Am. Chem. Soc.* **2006**, *128*, 16971–16979.
- (72) Wilding, M. J. T.; Iovan, D. A.; Betley, T. A. High-Spin Iron Imido Complexes Competent for C-H Bond Amination. *J. Am. Chem. Soc.* 2017, 139, 12043–12049.
- (73) Baek, Y.; Hennessy, E. T.; Betley, T. A. Direct Manipulation of Metal Imido Geometry: Key Principles to Enhance C-H Amination Efficacy. *J. Am. Chem. Soc.* **2019**, *141*, 16944–16953.
- (74) Kuijpers, P. F.; van der Vlugt, J. I.; Schneider, S.; de Bruin, B. Nitrene Radical Intermediates in Catalytic Synthesis. *Chem. Eur. J.* **2017**, 23, 13819–13829.
- (75) Wolczanski, P. T. Flipping the Oxidation State Formalism: Charge Distribution in Organometallic Complexes as Reported by Carbon Monoxide. *Organometallics* **201**7, *36*, 622–631.
- (76) (a) DiMucci, I. M.; Lukens, J. T.; Chatterjee, S.; Carsch, K. M.; Titus, C. J.; Lee, S. J.; Nordlund, D.; Betley, T. A.; MacMillan, S. N.; Lancaster, K. M. The Myth of d⁸ Copper(III). *J. Am. Chem. Soc.* **2019**, 141, 18508–18520. (b) DiMucci, I. M.; Titus, C. J.; Nordlund, D.; Bour, J. R.; Chong, E.; Grigas, D. P.; Hu, C. H.; Kosobokov, M. D.; Martin, C. D.; Mirica, L. M.; Nebra, N.; Vicic, D. A.; Yorks, L. L.; Yruegas, S.; MacMillan, S. N.; Shearer, J.; Lancaster, K. M. Scrutinizing formally Ni-IV centers through the lenses of core spectroscopy, molecular orbital theory, and valence bond theory. *Chem. Sci.* **2023**, 14, 6915–6929.